Cascade atom in high-Q cavity:
The spectrum for non-Markovian decay

B.J. Dalton[1] and B.M. Garraway[2]

[1] ARC Centre for Quantum-Atom Optics and Centre for Atom Optics and Ultrafast Spectroscopy,
Swinburne University of Technology, Melbourne, Victoria 3122, Australia
[2]Department of Physics and Astronomy, University of Sussex, Falmer, Brighton, BN1 9QH, United Kingdom
(Dated: February 1, 2008)

The spontaneous emission spectrum for a three level cascade configuration atom in a single mode high-Q cavity coupled to a zero temperature reservoir of continuum external modes is determined from the atom-cavity mode master equation using the quantum regression theorem. Initially the atom is in its upper state and the cavity mode empty of photons. Following Glauber, the spectrum is defined via the response of a detector atom. Spectra are calculated for the detector located inside the cavity (case A), outside the cavity end mirror (Case B—end emission), or placed for emission out the side of the cavity (Case C). The spectra for case A and case B are found to be essentially the same. In all the cases the predicted lineshapes are free of instrumental effects and only due to cavity decay. Spectra are presented for intermediate and strong coupling regime situations (where both atomic transitions are resonant with the cavity frequency), for cases of non-zero cavity detuning, and for cases where the two atomic transition frequencies differ. The spectral features for Cases B(A) and C are qualitatively similar, with six spectral peaks for resonance cases and eight for detuned cases. These general features of the spectra can be understood via the dressed atom model. However, Case B and C spectra differ in detail, with the latter exhibiting a deep spectral hole at the cavity frequency due to quantum interference effects.

I. INTRODUCTION

Since the original paper of Purcell [1] the modification of atomic radiative decay due to the presence of optical and microwave cavities, photonic band gap (PBG) materials has become a familiar topic of study in quantum optics. The presence of these systems structures the modes of the electromagnetic (EM) field, resulting in situations where the mode frequency dependences of the mode density or the atom-field coupling constants (or both) are changed from the free space situation. The quantum EM field acts as a structured reservoir whose behaviour depends on the product of the mode density with the square of the coupling constants—the reservoir structure functions. If the reservoir structure functions vary slowly with mode frequency, the corresponding reservoir correlation time may be short compared to the time scale over which the atomic state changes, and the atomic density operator satisfies a Markovian master equation. This results in the irreversible decay of excited atomic state populations, though with a decay rate different to that for radiative decay in free space. This regime is characterised by a weak coupling between the atom and the EM field. On the other hand, if the reservoir structure functions vary rapidly with mode frequency, the corresponding reservoir correlation time may be long compared to the time scale over which the atomic state changes, and the atomic density operator no longer satisfies a Markovian master equation. A reversible oscillatory decay of excited atomic state populations results, with a period related to the atom-field coupling constant. This regime is characterised by a strong coupling between the atom and the EM field.

There are a large variety of effects associated with atoms in structured EM fields, including modifications to the spontaneous emission, fluorescence and probe absorption spectra, and comprehensive surveys may be found in several reviews, for example [2, 3, 4]. Amongst the many effects is the modification of the spectrum of the radiation emitted when an excited atom decays into initially empty field modes. It has been known from the early days of quantum optics that for an initially excited two-level atom (TLA) in free space, this so-called spontaneous emission (SE) spectrum is a Lorentzian centred around the atomic transition frequency and with a width given by the excited atom decay rate [5]. In the weak coupling regime the spectrum will remain Lorentzian, but with a modified width reflecting the changed atomic decay rate. The situation changes qualitatively for the strong coupling regime, with the spectrum no longer remaining Lorentzian. The essential physics for a TLA coupled to a single mode cavity in the strong coupling regime can be described via the Jaynes-Cummings model [6], where the energy eigenstates allowing for the atom-cavity mode coupling are the so-called dressed atom states [7].

The first calculation for the SE spectrum for a TLA in an ideal lossless cavity was carried out by Sanchez-Mondragon et al. [8]. Using a Heisenberg equation of motion approach and determining the spectrum from the two-time correlation function for the atomic dipole operator, they found a double peaked spectrum with a separation between peaks given by the so-called one-photon Rabi frequency, that is the Rabi frequency associated with one photon in the cavity mode. Line shapes were associated with the spectrometer bandwidth [9], since no cavity bandwidth was included. Another early calculation for a TLA in a high-Q cavity was that of Agarwal [10], who used the dressed atom model to predict

the SE and weak probe absorption spectra. This article determines the SE spectrum for different positions of the spectrometer, the spectrum associated with sideways emission via direct SE being given in terms of the two-time dipole correlation function, whilst the spectrum associated with end emission via the cavity output mirror is given in terms of the two-time correlation function for cavity creation and annihilation operators. Although qualitatively similar in exhibiting vacuum Rabi frequency splitting, the spectra are quantitatively different. The SE spectra shown had lineshapes determined for the situation where the spectrometer bandwidth was large compared to the cavity decay rate. Non-Lorentzian SE spectra were also found by Lewenstein et al. [11] for emission from a TLA into both high Q cavities and PBG systems, here an essential states approach was used and the spectrum defined in terms of the long time probability for finding one photon in a cavity or background mode. Using a master equation and quantum regression theorem [12] approach, Carmichael et al. [13] took into account both cavity damping and spontaneous emission damping to determine the side emission SE spectrum for a TLA in a high-Q cavity from the two-time dipole correlation function, based on a zero bandwidth spectrometer. Further discussion and references on the theory of the SE spectrum for a TLA in a high-Q cavity are given by Childs et al. [14] and Carmichael et al. [15] in the review [2].

No *direct* experimental measurements of the SE spectrum for a single TLA in a high-Q cavity appear to have been carried out. However there are related experiments in the strong coupling regime, such as on the absorption spectrum for a weak probe field that demonstrates single atom vacuum Rabi splitting [16, 17], or single atom Rabi oscillations [18], or the collapse and revival experiments with a single TLA [19] that demonstrate cavity mode quantization [20, 21]. All these measurements can be interpreted in terms of the Jaynes-Cummings model [6] and the associated dressed atom states [7]. The direct measurement of SE spectra would probably only be possible in the optical regime, since SE in the microwave regime would be too weak to detect. For the case of a single TLA in a high-Q cavity or a PBG system which is also coupled to a strong laser field, there is an extensive literature dealing with the related spectra, in particular the spectra associated with resonance fluorescence or probe absorption. The work of Mollow [22] for the free space situation predicted a three-peaked (AC Stark effect) fluorescence spectrum, and a dispersion-like probe absorption spectrum. For a TLA in an ideal lossless cavity in a coherent state Agarwal et al. [23] predicted a large number of spectral lines in the fluorescence spectra, reflecting the contributions from the numerous dressed atom states involved. These spectra can also be interpreted via the dressed atom model, see the recent reviews [2, 3, 4].

In contrast to the case of the SE spectrum for a TLA in a high-Q cavity or a PBG system, the case of three level atoms (3LA) has received little attention. The SE

spectrum for a 3LA in a lambda configuration in a PBG system has been treated by John et al. [24] via the essential states approach for various detunings from the band gap edge, the spectrum (which shows doublet and window effects) being defined via the photon emission probability. Ashraf [25] determined the SE spectrum for a 3LA in a lambda configuration in an ideal lossless cavity using the dressed states approach, the spectrum (which shows a doublet structure reflecting the one photon Rabi frequency) being given via the two-time dipole correlation function. Line shapes were due to the spectrometer bandwidth. For a 3LA in a cascade configuration in a PBG system, Bay et al. [26] used the essential states approach to determine the SE spectrum for various detunings of one of the atomic transitions from the band gap edge, the latter (which is strongly non-Lorentzian) being defined via the photon emission probability. The treatment applies when the two atomic frequencies are quite distinct, enabling only one at a time to interact strongly with the PBG. Paspalakis et al. [27] treated the case of SE from a 3LA in a lambda configuration in a PBG system, using the same approach and spectrum definition as [24]. Similar spectral features were found, including the window not previously noted by John et al. The case of a 3LA in a cascade configuration in an ideal lossless cavity has been studied by Zhou et al. [28] using a dressed atom approach and both end and side SE spectra were determined. Line shapes were due to the spectrometer bandwidth, as no cavity damping was included. The cavity mode was resonant with the average of the atomic transition frequencies. For the situation where the two atomic transition frequencies were equal, six peaks were found in both the side emission and end emission SE spectra, though in the latter case two of these were negligible. When the two atomic transition frequencies differed, there were eight peaks in the side emission spectrum.

In a recent paper [29] we have considered the non-Markovian decay of a three level cascade atom with both transitions coupled to a single structured reservoir of quantized field modes for both a high-Q cavity and in a PBG system. Based on the approach given in [30] the dynamics of this system has been treated via the essential states approach, using Laplace transform methods applied to the coupled amplitude equations. Non-Markovian behaviour for the population dynamics of the atomic system was found, such as oscillatory decay for the high-Q cavity case and population trapping for the photonic band-gap case. A Markovian master equation approach was also applied, in which the atomic system was augmented by a small number of discrete quasimodes or pseudomodes, which in the quasimode treatment themselves undergo Markovian relaxation into a flat reservoir of continuum quasimodes. For the high-Q cavity case a single discrete quasimode was involved, for the PBG case two coupled discrete quasimodes were needed. The essential states and Markoff methods gave identical results, showing that complicated non-Markovian behaviour can be treated by enlarging the non-Markovian

system, thereby turning a non-Markovian problem into a Markovian one.

In the present paper we now consider the SE spectrum for the case of a cascade atom in a high-Q cavity. The spectrum is much richer than for the TLA case and quantum interference effects may now occur. Quantum coherence and interference phenomena are central in many applications of fundamental quantum optics results, and a comprehensive review of such effects may be found in a special issue of this journal on quantum inteference [31]. Unlike previous work, we will consider the case of an ideal spectrometer with zero bandwidth in order to display the actual SE spectral line shapes without these being masked by instrumental effects. A master equation approach incorporating cavity decay will be used to evaluate the spectra via the quantum regression theorem. Both end (Case A(B)) and side (Case C) SE spectra will be calculated, and we aim to exhibit the expected quantum interference effects that can occur in a cascade system. We will show that the spectrum in both cases are given in terms of the Laplace transforms of both the atom-cavity mode density matrix elements and the evolution operator matrix elements.

Before developing the mathematical formalism it may be useful to consider the physical processes that can be involved in the decay of the cascade atom in a high-Q cavity and the registration of a photon arrival in a suitable detector—this will enable possible interference effects to be identified. In a cascade atom initially in its upper state $|2\rangle$ and coupled to a high Q cavity empty of photons, two photons can be emitted before the atom makes a transition to its lowest state $|0\rangle$ via the intermediate state $|1\rangle$. If there is a detector atom weakly coupled to the atom-cavity mode system and prepared in its lower state $|A\rangle$, the detector atom could absorb one of these photons and make a transition to its upper state $|B\rangle$. Following the approach of Glauber [32] the overall tran-

sition probability for the $|A\rangle \rightarrow |B\rangle$ process considered as a function of the detector atom transition frequency ω may be used for an operational definition of the spontaneous emission spectrum for this cascade atom in a high Q cavity—the cavity mode being coupled to empty external modes via the cavity mirror. Since the detector atom is only weakly coupled we need only consider processes with a single $|A\rangle \rightarrow |B\rangle$ transition. Also, steps where a photon is created in an external mode would not be reversible. On the other hand if the atom-cavity mode coupling is strong, atomic transitions accompanied by photon number changes in the cavity mode may be reversible. If we consider the case (*Case A*) where the detector atom is placed inside the cavity, then the photon causing the detector atom transition must have come from the cavity mode. However photons in the cavity mode can also be transferred to an external mode via loss through the cavity mirror, and if one photon is used to cause the $|A\rangle \rightarrow |B\rangle$ transition in the detector atom, the other will be transferred to an external mode. We consider states of the combined detector atom, cavity mode, cascade atom, external mode system of the product form $|D; n; \nu; m\rangle$, where $D = A, B$; $n = 0, 1, 2, \ldots$; $\nu = 0, 1, 2$; $m = 0, 1, 2, \ldots$ specify the detector atom state, the cavity photon number, the atomic state and the photon number for a specific external mode respectively. Then the overall process in which the cascade atom changes from upper state $|2\rangle$ to lowest state $|0\rangle$, the detector atom changes from lower state $|A\rangle$ to upper state $|B\rangle$ and one photon appears in a specific external mode, whilst the cavity mode is initially and finally empty of photons is denoted $|A; 0; 2; 0\rangle \rightarrow |B; 0; 0; 1\rangle$. However this overall process involving the overall emission of two photons (one being absorbed by the detector atom, the other appearing in an external mode) has a number of different quantum pathways:

$$|A; 0; 2; 0\rangle \leftrightarrow |A; 1; 1; 0\rangle \rightsquigarrow |A; 0; 1; 1\rangle \leftrightarrow |A; 1; 0; 1\rangle \rightarrow |B; 0; 0; 1\rangle$$

$$|A; 0; 2; 0\rangle \leftrightarrow |A; 1; 1; 0\rangle \rightarrow |B; 0; 1; 0\rangle \leftrightarrow |B; 1; 0; 0\rangle \rightsquigarrow |B; 0; 0; 1\rangle$$

$$|A; 0; 2; 0\rangle \leftrightarrow |A; 1; 1; 0\rangle \leftrightarrow |A; 2; 0; 0\rangle \rightsquigarrow |A; 1; 0; 1\rangle \rightarrow |B; 0; 0; 1\rangle$$

$$|A; 0; 2; 0\rangle \leftrightarrow |A; 1; 1; 0\rangle \leftrightarrow |A; 2; 0; 0\rangle \rightarrow |B; 1; 0; 0\rangle \rightsquigarrow |B; 0; 0; 1\rangle \tag{1}$$

Reversible atom-cavity mode transitions are designated $\leftrightarrow$, irreversible cavity-external mode transitions $\rightsquigarrow$ and weak detector atom transitions $\rightarrow$. In addition, each of the reversible steps in the above pathways may involve further pathways if the atom-cavity mode coupling is strong. For example, the first pathway

$$|A; 0; 2; 0\rangle \leftrightarrow |A; 1; 1; 0\rangle \rightsquigarrow |A; 0; 1; 1\rangle \leftrightarrow |A; 1; 0; 1\rangle \rightarrow |B; 0; 0; 1\rangle \tag{2}$$

could branch into two different sub-pathways

$$|A; 0; 2; 0\rangle \leftrightarrow |A; 1; 1; 0\rangle \leftrightarrow |A; 2; 0; 0\rangle \leftrightarrow |A; 1; 1; 0\rangle \rightsquigarrow |A; 0; 1; 1\rangle \leftrightarrow |A; 1; 0; 1\rangle \rightarrow |B; 0; 0; 1\rangle \tag{3}$$

$$|A; 0; 2; 0\rangle \leftrightarrow |A; 1; 1; 0\rangle \leftrightarrow |A; 0; 2; 0\rangle \leftrightarrow |A; 1; 1; 0\rangle \rightsquigarrow |A; 0; 1; 1\rangle \leftrightarrow |A; 1; 0; 1\rangle \rightarrow |B; 0; 0; 1\rangle \tag{4}$$

The possibilities for branching are endless. The tran-

sition amplitudes for all these different pathways (and

sub-pathways) are added to form the overall transition amplitude, and hence the transition probability would be expected to exhibit quantum interference effects. Thus the spontaneous emission spectrum for a three level cascade atom should demonstrate interesting interference phenomena.

Of course there will also be a detection processes in which the cascade atom changes from upper state $|2\rangle$ to intermediate state $|1\rangle$, the detector atom changes from lower state $|A\rangle$ to upper state $|B\rangle$ but no photon appears

in a specific external mode, whilst the cavity mode is initially and finally empty of photons. This is denoted $|A;0;2;0\rangle \rightarrow |B;0;1;0\rangle$ and involves only one photon emission, the emitted photon being absorbed by the detector atom. Here

$$|A;0;2;0\rangle \leftrightarrow |A;1;1;0\rangle \rightarrow |B;0;1;0\rangle \qquad (5)$$

is the only quantum pathway, though again there are numerous sub-pathways such as

$$|A;0;2;0\rangle \;\leftrightarrow\; |A;1;1;0\rangle \leftrightarrow |A;2;0;0\rangle \leftrightarrow |A;1;1;0\rangle \rightarrow |B;0;1;0\rangle$$
$$|A;0;2;0\rangle \;\leftrightarrow\; |A;1;1;0\rangle \leftrightarrow |A;0;2;0\rangle \leftrightarrow |A;1;1;0\rangle \rightarrow |B;0;1;0\rangle \qquad (6)$$

if the atom-cavity mode coupling is strong . For this overall process there still may be quantum interference effects. Similar processes to these would apply if the only atomic states considered were $|2\rangle$ and $|1\rangle$, with the coupling to the lower state $|0\rangle$ being set to zero, and sub-pathways involving $|0\rangle$ excluded. In all these cases the amplitudes for different sub-pathways would combine to produce an overall transition amplitude, and hence interference effects giving maxima and minima in the detection probability (spectrum) could occur. Whether these interference effects can be be demonstrated directly via altering the system coupling constants, detunings etc. is a separate issue.

A similar discussion can be presented for the case where the detector atom is placed just outside the cavity mirror (*Case B*) to detect end emission, or where the detector atom is placed outside the cavity to detect the weak side emission (*Case C*). In case B it is the external mode photon absorption that is associated with the detector atom transition, in case C it is the transition in the cascade atom itself, so the details of the discussion will differ for these two cases.

In Section II the general features of the quasimode description used to treat the cascade atom-cavity mode system are covered, along with a brief outline of the approach for defining the spectrum and how the quantum regression theorem is used in the calculations. Section III covers the master equation for the cascade atom-cavity mode system, the related evolution operator and their determination in terms of Laplace transforms. Expressions for the SE spectra for three different positions of the spectrometer atom—inside the cavity (Case A), outside the cavity to detect end emission (Case B) and outside the cavity to detect side emission (Case C) are given in Section III. Numerical results for the SE spectrum for the cascade atom in a high-Q cavity are presented in Section IV and conclusions given in Section V. Details are presented in the Appendices.

II. GENERAL THEORY

A. Atom-quasimode system

The general system of interest is a radiating atom with energy states $|E_\alpha\rangle$ coupled to a discrete set of quasimodes i of the quantum EM field, which in turn are coupled to a continuum set of quasimodes Δ. The Hamiltonian $\widehat{H}$ for the atom-quasimodes system is given as the sum of the atomic Hamiltonian $\widehat{H}_A$, the quasimodes Hamiltonian $\widehat{H}_Q$ and an interaction between the atom and quasimodes $\widehat{H}_{AQ}$ [30]

$$\widehat{H} = \widehat{H}_A + \widehat{H}_Q + \widehat{H}_{AQ}, \qquad (7)$$

where

$$\widehat{H}_A \;=\; \sum_\alpha \hbar\omega_\alpha \,|E_\alpha\rangle\,\langle E_\alpha| \qquad (8)$$

$$\widehat{H}_Q \;=\; \sum_i \hbar\nu_i\,\widehat{a}_i^\dagger\widehat{a}_i + \sum_{i\neq j}\hbar V_{ij}\,\widehat{a}_i^\dagger\widehat{a}_j$$
$$+ \int d\Delta\,\rho_C(\Delta)\,\hbar\Delta\,\widehat{b}(\Delta)^\dagger\widehat{b}(\Delta)$$
$$+ \sum_i \int d\Delta\,\rho_C(\Delta)\,(\hbar W_i(\Delta)\widehat{a}_i^\dagger\widehat{b}(\Delta) + H.C.)$$

$$(9)$$

$$\widehat{H}_{AQ} \;=\; \sum_{E_\alpha > E_\beta}\sum_i (\hbar\lambda_{i;\alpha\beta}^*\,\widehat{a}_i\,|E_\alpha\rangle\,\langle E_\beta| + H.C.). \quad (10)$$

In these equations $E_\alpha = \hbar\omega_\alpha$ is the atomic energy, ν_i and Δ are the frequencies of the discrete and continuum quasimodes, $\widehat{a}_i^\dagger, \widehat{a}_i$ and $\widehat{b}(\Delta)^\dagger, \widehat{b}(\Delta)$ are the standard creation, annihilation operators for these quasimodes with commutation rules $[\widehat{a}_i,\widehat{a}_j^\dagger] = \delta_{ij}, [\widehat{b}(\Delta),\widehat{b}(\Delta')^\dagger] = \delta(\Delta - \Delta')/\rho_C(\Delta)$, $\hbar V_{ij}$ is the coupling energy between discrete quasimodes, $\hbar W_i(\Delta)$ describes the coupling between discrete and continuum quasimodes and $\hbar\lambda_{i;\alpha\beta}$ specifies the

coupling between the discrete quasimode and the atomic transition between states $|E_\alpha\rangle, |E_\beta\rangle$. All interactions are given via the rotating wave approximation. The continuum mode density is $\rho_C(\Delta)$.

In the case where $W_i(\Delta)$ and $\rho_C(\Delta)$ are slowly varying functions of the continuum quasimode frequency, the system consisting of the atom plus discrete quasimodes is described by a reduced density operator $\widehat{\rho}$ satisfying a Markovian master equation [30]

$$\frac{\partial}{\partial t}\widehat{\rho} = -\frac{i}{\hbar}[\widehat{H}_S, \widehat{\rho}] + \sum_{ij} \pi \rho_C W_i W_j^* ([\widehat{a}_j, \widehat{\rho}\,\widehat{a}_i^\dagger] + [\widehat{a}_j\,\widehat{\rho}, \widehat{a}_i^\dagger]),$$

(11)

where the first term involves the Hamiltonian for the atom-discrete quasimode system $\widehat{H}_S$ and the second term describes relaxation due to the interaction between the discrete quasimodes and a reservoir consisting of the continuum quasimodes. The Hamiltonian $\widehat{H}_S$ is given by

$$\widehat{H}_S = \widehat{H}_A + \widehat{H}_{QD} \qquad (12)$$

$$\widehat{H}_{QD} = \sum_i \hbar\nu_i\,\widehat{a}_i^\dagger\widehat{a}_i + \sum_{i\neq j} \hbar V_{ij}\,\widehat{a}_i^\dagger\widehat{a}_j. \qquad (13)$$

B. Spectrum

The spectrum $S(\omega)$ is defined operationally [32, 33] in terms of the long time transition probability to the upper state $|B\rangle$ for a two-level atom detector with transition frequency ω that is initially in its lower state $|A\rangle$ and which is weakly coupled to the EM field, and where the final state of the atom-quasimode system is unobserved. The Hamiltonian $\widehat{\mathcal{H}}$ for the combined system of detector atom and the radiating atom-quasimode system is then

$$\widehat{\mathcal{H}} = \widehat{H} + \widehat{H}_D + \widehat{V}_{SD} \qquad (14)$$

where the Hamiltonians for the detector atom and its coupling to the radiating atom-quasimode system are

$$\widehat{H}_D = \hbar\omega\widehat{S}_Z \qquad (15)$$

$$\widehat{V}_{SD} = \hbar(\widehat{V}_+\widehat{S}_- + \widehat{V}_-\widehat{S}_+). \qquad (16)$$

Here $\widehat{S}_+ = |B\rangle\langle A|$, $\widehat{S}_- = |A\rangle\langle B|$ and $\widehat{S}_Z = \frac{1}{2}(|B\rangle\langle B| - |A\rangle\langle A|)$ are the usual atomic spin operators. The operators $\widehat{V}_+$, $\widehat{V}_-$ depend on where the detector atom is situated and hence what region of the quantum EM field it samples. In all cases $\widehat{V}_+$, $\widehat{V}_-$ are proportional to the negative, positive frequency components $\widehat{\mathcal{E}}_-$, $\widehat{\mathcal{E}}_+$ of the electric field operator at the detector atom. For the case where the detector atom is situated inside a high Q cavity or is situated outside the output mirror, the EM field can be conveniently described in terms of quasimodes [30, 34, 35]. In the case (Case A) when it is inside a high Q cavity—see figure 1—the detector atom samples the discrete quasimodes, in another case (Case B) when it is situated outside a high Q cavity to detect end emission—see figure 1—it samples the continuum quasimodes. For
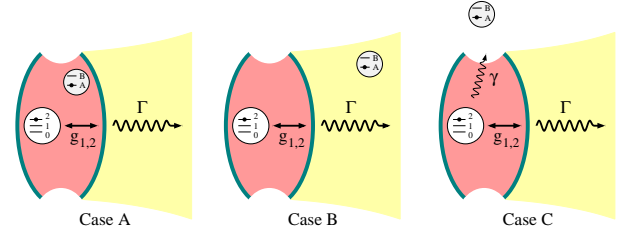

FIG. 1: The cascade atom in a high-Q cavity with the detector atom in various locations. In Case A the detector atom is inside the cavity, in Case B it is outside the cavity output mirror and positioned to detect end emission and in Case C it is outside the cavity positioned to detect side emission.

cases when the detector atom is situated outside a high Q cavity to detect side emission—see figure 1 (Case C)—the EM field is conveniently described in terms of true modes [36, 37]. In the three cases we have

$$\widehat{V}_- = \sum_i \mu_i^* \widehat{a}_i = (\widehat{V}_+)^\dagger \qquad \qquad Case\ A \qquad (17)$$

$$\widehat{V}_- = \int d\Delta\,\rho_C(\Delta)\,\mu^*(\Delta)\widehat{b}(\Delta) = (\widehat{V}_+)^\dagger$$

$$Case\ B \qquad (18)$$

$$\widehat{V}_- = \sum_{E_\alpha < E_\beta} R_{\alpha\beta}^* \,|E_\alpha\rangle\langle E_\beta| = (\widehat{V}_+)^\dagger$$

$$Case\ C\,, \qquad (19)$$

where μ_i, $\mu(\Delta)$ and $R_{\alpha\beta}$ are weak coupling constants. For simplicity we will ignore retardation effects—these could be included by incorporating the position of the detector atom in μ_i^*, $\mu^*(\Delta)$ and $R_{\alpha\beta}$ and that of the radiating atom in the $\lambda_{i;\alpha\beta}^*$, and by arranging the detector atom to begin responding when the emitted EM field first reaches it. In Case C the expression for $\widehat{V}_-$ is based on the long distance radiating atom contribution to the EM field positive frequency component $\widehat{\mathcal{E}}_+$ being related to the electric dipole operator of the radiating atom (ignoring the free evolution term, which gives a zero contribution to the spectrum), and $\widehat{V}_-$ can be expressed in terms of the downward atomic transition operators $|E_\alpha\rangle\langle E_\beta|$ $(E_\alpha < E_\beta)$.

If the initial state of the atom-quasimodes system is a pure state $|\Phi_i\rangle$ and the detector is in state $|A\rangle$ then the probability amplitude for the transition to an atom-quasimode system state $|\Phi_f\rangle$ and the detector in state $|B\rangle$ is given by

$$A_{FI} = \langle F|\widehat{U}(t)|I\rangle, \qquad (20)$$

with $|I\rangle = |\Phi_i\rangle\,|A\rangle$ and $|F\rangle = |\Phi_f\rangle\,|B\rangle$ and $\widehat{U}(t) = \exp(-i\widehat{\mathcal{H}}t/\hbar)$ the evolution operator for the combined atom-quasimode-detector system. If the atom-quasimode system is initially in a mixed state with density operator $\widehat{\rho}_I = \sum_i p_i |\Phi_i\rangle\langle\Phi_i|$ then the transition

probability to the upper detector atom state and to any final state of the atom-quasimode system is given by

$$P_{BA} = \sum_f \sum_i p_i |\langle F| \widehat{U}(t) |I\rangle|^2, \qquad (21)$$

and for long times t this will be taken as the un-normalised spectrum $S(\omega)$.

A straightforward quantum treatment [38] which involves expressing the evolution operator as a sum of terms with increasing orders of $\widehat{V}_{SD}$ then gives

$$\langle F| \widehat{U}(t) |I\rangle = \frac{1}{i\hbar} \exp(-i\omega t) \int_0^t dt_1 \exp(i\omega t_1) \langle \Phi_f| \exp(-i\widehat{\mathcal{H}}(t - t_1)/\hbar)\widehat{V}_- \exp(-i\widehat{\mathcal{H}}(t_1)/\hbar) |\Phi_i\rangle, \qquad (22)$$

and finally as $t \to \infty$

$$\begin{aligned} S(\omega) &= \frac{1}{\hbar^2} \iint_0^\infty dt_1 dt_2 \exp i\omega(t_1 - t_2) \\ &\times Tr\left(\widehat{\rho}_I \widehat{V}_+(t_2) \widehat{V}_-(t_1)\right), \end{aligned} \qquad (23)$$

where

$$\begin{aligned} \widehat{V}_-(t) &= \exp(+i\widehat{H}\,t/\hbar)\widehat{V}_-\exp(-i\widehat{H}\,t)/\hbar) \\ \widehat{V}_+(t) &= \exp(+i\widehat{H}\,t/\hbar)\widehat{V}_+\exp(-i\widehat{H}\,t)/\hbar) \\ &= (\widehat{V}_-(t))^\dagger \end{aligned} \qquad (24)$$

are the system Heisenberg picture operators associated with $\widehat{V}_-$ and $\widehat{V}_+$. The trace is over the radiating atom-quasimodes system. The expression for the spectrum is real, as expected. This approach defines the so-called *operational spectrum*.

A rather different approach to defining the spectrum is based on the essential states approximation. Here the state vector for the full atom and EM field modes system—the modes are still described via quasi-modes—is expanded in a basis set $|E_\alpha; n_i; m(\Delta)\rangle$ where n_i and $m(\Delta)$ are the numbers of photons in the ith discrete and Δ continuum quasimodes. Thus

$$\begin{aligned} |\Psi(t)\rangle &= \sum_\alpha \sum_{n_i} \int d\Delta\, \rho_C(\Delta) \sum_{m(\Delta)} b(E_\alpha; n_i; m(\Delta); t) \\ &\times \exp(-i\{\omega_\alpha + n_i\nu_i + m(\Delta)\Delta\}t) \\ &\times |E_\alpha; n_i; m(\Delta)\rangle, \end{aligned} \qquad (25)$$

with interaction picture amplitudes $b(E_\alpha; n_i; m(\Delta); t)$. The long time one photon emission spectrum would be defined in this approach via the long time probability of finding one photon in a continuum mode of frequency Δ

$$S_I(\Delta) = \sum_\alpha \sum_{n_i} |b(E_\alpha; n_i; 1(\Delta); \infty)|^2, \qquad (26)$$

in which the continuum quasimode frequency acts as the spectral variable. This approach may be referred to as defining the *ideal spectrum*, corresponding to quantities arising naturally from fundamental considerations of what can in principle be measured in quantum mechanics, rather than to the analysis of the behaviour of a model spectrometer. An alternative definition of an ideal spectrum [39] could be based on true mode states—which also form a continuum—rather than continuum quasi-modes states. The interrelationship between the different approaches to defining spectra has been considered by Cresser [33]. Calculations of the ideal spectrum would involve solving the coupled amplitude equations.

C. Quantum regression theorem

Determination of the operational spectrum requires the evaluation of two-time correlation functions, and here the quantum regression theorem is used. The usual statement of the quantum regression theorem [12, 40, 41] is that for a system operator $\widehat{Y}_i(t)$ in the Heisenberg picture whose average satisfies the linear equation ($t \geqslant 0$)

$$\frac{d}{dt}\left\langle \widehat{Y}_i(t)\right\rangle = \sum_j G_{ij}(t)\left\langle \widehat{Y}_j(t)\right\rangle, \qquad (27)$$

with matrix elements $G_{ij}(t)$, then we can assert that the two time correlation functions ($\tau \geqslant 0$) satisfy a similar linear equation involving the same matrix elements

$$\frac{d}{d\tau}\left\langle \widehat{Y}_i(t+\tau)\widehat{Y}_l(t)\right\rangle = \sum_j G_{ij}(\tau)\left\langle \widehat{Y}_j(t+\tau)\widehat{Y}_l(t)\right\rangle \qquad (28)$$

$$\frac{d}{d\tau}\left\langle \widehat{Y}_l(t)\widehat{Y}_i(t+\tau)\right\rangle = \sum_j G_{ij}(\tau)\left\langle \widehat{Y}_l(t)\widehat{Y}_j(t+\tau)\right\rangle. \qquad (29)$$

A useful result giving the two time correlation function $\left\langle \widehat{S}_{\beta\alpha}(t+\tau)\widehat{S}_{\delta\gamma}(t)\right\rangle$ for system transition operators in terms of matrix elements of the evolution operator and density matrix elements [41] can be derived from this form of the quantum regression theorem by considering the case where $\widehat{Y}_i$ is a system transition operator $\widehat{Y}_i \equiv$

$\widehat{S}_{\beta\alpha} = |\beta\rangle\langle\alpha|$. In this case $\left\langle\widehat{Y}_i(t)\right\rangle \equiv \left\langle\widehat{S}_{\beta\alpha}(t)\right\rangle = \rho_{\alpha\beta}(t)$, the density matrix element which satisfies the master equation. In general we can write the solution to the master equation in terms of matrix elements $U_{\alpha\beta;\,\gamma\delta}(t)$ of the evolution operator

$$\rho_{\alpha\beta}(t) = \sum_{\gamma\delta} U_{\alpha\beta;\,\gamma\delta}(t)\,\rho_{\gamma\delta}(0). \qquad (30)$$

We then can show that for $(t \geqslant 0, \tau \geqslant 0)$ the two important results

$$\left\langle\widehat{S}_{\beta\alpha}(t+\tau)\widehat{S}_{\delta\gamma}(t)\right\rangle = \sum_{\mu} U_{\alpha\beta;\,\delta\mu}(\tau)\,\rho_{\gamma\mu}(t) \quad (31)$$

$$\left\langle\widehat{S}_{\beta\alpha}(t)\widehat{S}_{\delta\gamma}(t+\tau)\right\rangle = \sum_{\mu} U_{\gamma\delta;\,\mu\alpha}(\tau)\,\rho_{\mu\beta}(t). \quad (32)$$

These results give the two time correlation function $\left\langle\widehat{S}_{\beta\alpha}(t+\tau)\widehat{S}_{\delta\gamma}(t)\right\rangle$ for system transition operators in terms of matrix elements of the evolution operator and density matrix elements.

III. THREE LEVEL CASCADE ATOM IN SINGLE MODE CAVITY

A. Master equation

The master equation for a three level cascade atom in a single mode high Q cavity coupled to the reservoir of continuum quasimodes at zero temperature is given by

$$\frac{\partial}{\partial t}\widehat{\rho} = -\frac{i}{\hbar}[\widehat{H}_S, \widehat{\rho}] + \frac{1}{2}\Gamma([\widehat{a}, \widehat{\rho}\,\widehat{a}^\dagger] + [\widehat{a}\,\widehat{\rho}, \widehat{a}^\dagger]), \qquad (33)$$

where the Hamiltonian for the three level atom plus cavity mode system in the rotating wave approximation is

$$\begin{aligned} \widehat{H}_S = \ & \hbar\omega_c\widehat{a}^\dagger\widehat{a} + \hbar(\omega_0 - \overline{\delta})\widehat{\sigma}_{22} - \hbar(\omega_0 + \overline{\delta})\widehat{\sigma}_{00} \\ & + \hbar[\widehat{a}^\dagger(g_2\widehat{\sigma}_2^- + g_1\widehat{\sigma}_1^-) + (g_2\widehat{\sigma}_2^+ + g_1\widehat{\sigma}_1^+)\widehat{a}]. \end{aligned}$$
$$(34)$$

Here $\widehat{a}, \widehat{a}^\dagger$ are the mode annihilation, creation operators for the single cavity quasimode with frequency ω_c. The operators $\widehat{\sigma}_2^+ = |2\rangle\langle1|$, $\widehat{\sigma}_2^- = |1\rangle\langle2|$, $\widehat{\sigma}_{1+} = |1\rangle\langle0|$, $\widehat{\sigma}_{1-} = |0\rangle\langle1|$ and $\widehat{\sigma}_{22}, \widehat{\sigma}_{11}, \widehat{\sigma}_{00}$ are atomic transition and population operators respectively, involving the upper state $|2\rangle$, the intermediate state $|1\rangle$ and the lower state $|0\rangle$. The lower $(1 \leftrightarrow 0)$ and upper $(2 \leftrightarrow 1)$ atomic transition frequencies are ω_1, ω_2 respectively. The average atomic transition frequency is ω_0 and $\overline{\delta}$ is half the difference between lower and upper transition frequencies. Thus $\omega_0 = (\omega_1 + \omega_2)/2$, $\overline{\delta} = (\omega_1 - \omega_2)/2$. The atomic term in the Hamiltonian is based on adding a constant $\lambda(\widehat{\sigma}_{22} + \widehat{\sigma}_{11} + \widehat{\sigma}_{00})$ to the original Hamiltonian so as to make the energy of the intermediate state $|1\rangle$ equal to zero. The atomic states are illustrated in figure 2, along
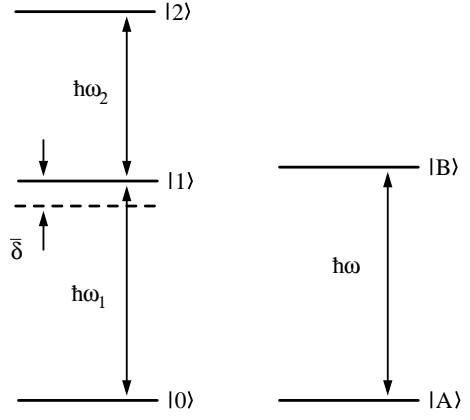

FIG. 2: Energy levels and energy differences in the three level cascade atom (left). The offset $\overline{\delta}$ represents the difference between the energy of level 1 and the midpoint between levels 0 and 2. The energy levels for the two state detector atom are also shown (right).

with the states of the detector atom. The one photon Rabi frequencies are g_2 and g_1 for the two transitions and Γ is the cavity decay rate, where we have used the notation $\lambda_{21} \to g_2$, $\lambda_{10} \to g_1$. The coupling constants g_1 and g_2 are proportional to the scalar product of the vector dipole matrix elements $\langle2|\,\widehat{\underset{\rightarrow}{d}}\,|1\rangle$, $\langle1|\,\widehat{\underset{\rightarrow}{d}}\,|0\rangle$ between the upper and intermediate states or the intermediate and lower states with the polarization unit vector for the cavity quasimode, and by a suitable choice of phase can be taken as real and positive. The reduced density operator is $\widehat{\rho}$. In terms of the flat continuum mode density ρ_C and discrete-continuum quasimodes coupling constant W, we have $\Gamma = 2\pi\rho_C|W|^2$. At zero temperature the continuum quasimodes are empty of photons. In the present case the atomic spontaneous emission rate γ into sideways EM field modes will be ignored in comparison to the cavity loss rate Γ. Thus we have $\Gamma \gg \gamma$. The case of non-negligible γ is discussed by [13] for the case of a two level atom.

For density matrix elements in the basis $|n;\nu\rangle$ (where $n = 0, 1, 2, \ldots$ is the cavity photon number and $\nu = 2, 1, 0$ specifies the upper, intermediate, and lowest atomic states) the master equation can be used to derive a set of coupled linear equations for the density matrix elements $\rho_{n\nu;\,m\mu}$ in which the coefficients depend on the cavity frequency ω_c, the detuning δ between the cavity frequency and the average atomic transition frequency $(\delta = \omega_c - \omega_0)$, the half difference between lower and upper transition frequencies $\overline{\delta}$, the coupling constants g_1, g_2 and the cavity decay rate Γ. The coupled density matrix equations are set out in a suitable form in Appendix A. The equations make up almost independent coupled sets of density matrix elements, if coupling only via the reversible processes associated with g_1, g_2 is considered. In general we designate the (n, m) set for all n, m to include the density matrix element $\rho_{n0;\,m0}$ (associated with the atom being in the lowest state $|0\rangle$) and any density

matrix elements coupled to it via reversible processes associated with the atom-cavity mode interaction terms. As we will see, relaxation due to cavity decay Γ couples a set (n, m) to other sets.

The sets with $(n, m \geqslant 2)$ consist of 9 elements— $\rho_{\overline{n-2}; \overline{m-2}2}$, $\rho_{\overline{n-2}; \overline{m-1}1}$, $\rho_{\overline{n-2}; m0}$, $\rho_{\overline{n-1}; \overline{m-2}2}$, $\rho_{\overline{n-1}; \overline{m-1}1}$, $\rho_{\overline{n-1}; m0}$, $\rho_{n0; \overline{m-2}2}$, $\rho_{n0; \overline{m-1}1}$ and $\rho_{n0; m0}$ and may be represented as a 1×9 column matrix

$$\rho(n, m) = \begin{bmatrix} \rho_{\overline{n-2}; \overline{m-2}2} \\ \rho_{\overline{n-2}; \overline{m-1}1} \\ \rho_{\overline{n-2}; m0} \\ \rho_{\overline{n-1}; \overline{m-2}2} \\ \rho_{\overline{n-1}; \overline{m-1}1} \\ \rho_{\overline{n-1}; m0} \\ \rho_{n0; \overline{m-2}2} \\ \rho_{n0; \overline{m-1}1} \\ \rho_{n0; m0} \end{bmatrix} . \quad (35)$$

This set is based on the three states of the form $|\overline{n-2}; 2\rangle$, $|\overline{n-1}; 1\rangle$ and $|n; 0\rangle$ $(n \geqslant 2)$ which are coupled via the reversible processes associated with the atom-cavity mode interaction. However the terms arising from the irreversible processes associated with the relaxation term $\Gamma \hat{a} \hat{\rho} \hat{a}^{\dagger}$ couple in $\rho_{\overline{n-1}2; \overline{m-1}2}$, $\rho_{\overline{n-1}2; m1}$, $\rho_{\overline{n-1}2; \overline{m+1}0}$, $\rho_{n1; \overline{m-1}2}$, $\rho_{n1; m1}$, $\rho_{n1; \overline{m+1}0}$, $\rho_{\overline{n+1}0; \overline{m-1}2}$, $\rho_{\overline{n+1}0; m1}$ and $\rho_{\overline{n+1}0; \overline{m+1}0}$, which are the density matrix elements in the $(n+1, m+1)$ set. Such irreversible processes are of the form $|n+1; \nu\rangle \rightarrow |n; \nu\rangle$ and these link in the three states $|\overline{n-1}; 2\rangle$ $|n; 1\rangle$ and $|\overline{n+1}; 0\rangle$ on which are based the $(n+1, m+1)$ set of density matrix elements.

Special consideration is required for the density matrix elements associated with the state $|0; 0\rangle$ (where there are no cavity photons and the atom is in the lowest state). This state is not coupled to other states via the atom-cavity mode reversible interaction processes, and its only link with other states is via the irreversible $|1; 0\rangle \rightarrow |0; 0\rangle$ relaxation process. The density matrix equations associated with the $|0; 0\rangle$ state take on special forms. Similarly, special consideration is required for the density matrix elements associated with the states $|0; 1\rangle$ and $|1; 0\rangle$ (where there are no cavity photons and the atom is in the intermediate state or there is one cavity photon and the atom is in the lowest state). These states are coupled together but not coupled to other states via the atom-cavity mode reversible interaction processes. Their only link with other states is via the irreversible $|1; 1\rangle \rightarrow |0; 1\rangle$ and $|2; 0\rangle \rightarrow |1; 0\rangle$ relaxation processes, and $|1; 0\rangle$ is linked to $|0; 0\rangle$ via the $|1; 0\rangle \rightarrow |0; 0\rangle$ relaxation process. The density matrix equations associated with the $|0; 1\rangle$ and $|1; 0\rangle$ states also take on special forms. We still find that the density matrix elements break up into separate coupled sets associated with the reversible atom-cavity mode interaction processes. Following the general procedure for designating the sets via the photon quantum numbers n, m associated with the density matrix element $\rho_{n0; m0}$ included in the set, the $(0, 0)$ set only contains the single density matrix element $\rho_{00; 00}$,

the $(0, 1)$ set contains two elements $\rho_{00; 01}, \rho_{00; 10}$, with the $(1, 0)$ set also containing two elements $\rho_{01; 00}, \rho_{10; 00}$. The $(0, 2)$ set contains three elements $\rho_{00; 02}, \rho_{00; 11}$ and $\rho_{00; 20}$, the $(2, 0)$ set also contains three elements $\rho_{02; 00}, \rho_{11; 00}$ and $\rho_{20; 00}$. Next there is the $(1, 1)$ set with four elements $\rho_{01; 01}, \rho_{01; 10}, \rho_{10; 01}$ and $\rho_{10; 10}$. Finally, there are two sets each with six elements, the $(1, 2)$ set consisting of $\rho_{01; 02}, \rho_{01; 11}, \rho_{01; 20}, \rho_{10; 02}, \rho_{10; 11}$ and $\rho_{10; 20}$, and the $(2, 1)$ set consisting of $\rho_{02; 01}, \rho_{02; 10}, \rho_{11; 01}, \rho_{11; 10}, \rho_{20; 01}$ and $\rho_{20; 10}$. Instead of there being 9 coupled equations as for the (n, m) set $(n, m \geqslant 2)$, there are $1, 2, 2, 3, 3, 4, 6$ and 6 coupled equations respectively for the $(0, 0), (0, 1), (1, 0), (0, 2), (2, 0), (1, 1), (1, 2)$ and $(2, 1)$ coupled sets. The complete sets of equations can be obtained from the master equation.

In all cases the density matrix equations can be conveniently be written in matrix form as

$$\frac{\partial}{\partial t} \rho(n, m) = -iA(n, m)\rho(n, m) + iB(n, m)\rho(n+1, m+1). \quad (36)$$

Expressions for the column vectors $\rho(n, m)$ and the matrices $A(n, m)$ and $B(n, m)$ which specify the coupling within the (n, m) set and the coupling to the $(n+1, m+1)$ set respectively, are set out in Appendix A for $(n, m \geqslant 2)$ and for the special $(0, 0)$, $(1, 0)$, $(1, 1)$, $(2, 1)$ and $(2, 2)$ sets.

Taking the Laplace transform of the equations for $\rho(n, m)$ gives

$$(s + iA(n, m)) \widetilde{\rho}(n, m) - iB(n, m) \widetilde{\rho}(n+1, m+1) = \rho(n, m, 0), \quad (37)$$

where s is the Laplace variable. The Laplace transform $\widetilde{A}(s)$ of a function $A(t)$ which is bounded for $t \geqslant 0$ is defined as for complex s in the right half plane via

$$\widetilde{A}(s) = \int_0^{\infty} dt \, \exp(-st) \, A(t) \qquad \text{Re } s \geqslant 0 \, . \quad (38)$$

The form of these equations indicates that if relaxation is *also* taken into account, *certain* collections of the $\rho(n, m)$ form independent coupled sets, the set containing a specific $\rho(n, m)$ also includes $\rho(n \pm 1, m \pm 1), \rho(n \pm 2, m \pm 2), \ldots, \rho(n \pm k, m \pm k), \ldots$, where k is a positive integer such that $n \pm k \geqslant 0, m \pm k \geqslant 0$. Thus $\rho(0, 0)$, $\rho(1, 1)$, $\rho(2, 2), \ldots$are all coupled, as are $\rho(1, 0)$, $\rho(2, 1)$, $\rho(3, 2), \ldots$etc. We see from the Laplace transform equations that if $\rho(n > N, m > M, 0)$ are all zero, then for $n > N$ and $m > M$ $(s + iA(n, m)) \widetilde{\rho}(n, m) - iB(n, m) \widetilde{\rho}(n+1, m+1) = 0$, and hence a solution to the equations given by $\widetilde{\rho}(n, m) = 0$ for $n > N$ and $m > M$ exists. Since linear first order equations have unique solutions, then $\rho(n, m, t) = 0$ for $n > N$ and $m > M$. This feature is the consequence of the relaxation processes occuring in one direction, with only the $|n+1; \nu\rangle \rightarrow |n; \nu\rangle$ transition (and not its reverse) taking place.

The solution to the density matrix equations at time t can be related to *any* initial density matrix in terms of

the matrices $U_{n,m::l,k}(t)$ representing the evolution super-operator $\widehat{\mathbf{U}}(t)$ for the master equation as

$$\rho(n,m,t) = \sum_{l,k} U_{n,m::l,k}(t)\,\rho(l,k,0), \qquad (39)$$

where the $U_{n,m::l,k}(t)$ satisfy the same matrix equations as $\rho(n,m,t)$, but have an initial condition involving a unit matrix E

$$U_{n,m::l,k}(0) = \delta_{(n,m),(l,k)}E_{(n,m)}. \qquad (40)$$

The dimensionality of the matrices $U_{n,m::l,k}(t)$ and $E_{(n,m)}$ depends on the sets (n,m) and (l,k). For example, if both (n,m) and (l,k) are such that $(n,m \geqslant 2)$ and $(l,k \geqslant 2)$ then the matrix is 9×9. On the other hand for $(n,m \geqslant 2)$ and $(l,k) = (0,1)$ or $(1,0)$ the matrix is 9×2, whilst if $(l,k) = (0,0)$ the matrix is 9×1. Other cases follow similar lines. In full for $(n,m \geqslant 2)$ and $(l,k \geqslant 2)$ the 81 matrix elements of $U_{n,m::l,k}(t)$ are $U_{(n\nu),(m\lambda)::(l\beta),(k\alpha)}(t)$, where $(n\nu) \equiv (\overline{n-2}2,\overline{n-1}1,n0),(m\lambda) \equiv (\overline{m-2}2,\overline{m-1}1,m0),(l\beta) \equiv (\overline{l-2}2,\overline{l-1}1,l0)$ and $(k\alpha) \equiv (\overline{k-2}2,\overline{k-1}1,k0)$. Other cases follow similar lines.

For the evolution matrices we can also obtain equations for their Laplace transforms, and we have

$$(s+iA(n,m))\,\widetilde{U}(n,m::l,k)$$
$$-iB(n,m)\,\widetilde{U}(n+1,m+1::l,k) = \delta_{(n,m),(l,k)}E_{(n,m)}. \qquad (41)$$

As we will see, Laplace transforms $\widetilde{U}(n,m::l,k)$ occur in the final expression for the spectrum. Note that as the $\rho(n,m)$ form independent coupled sets with relaxation only linking neighbouring sets (n,m) and $(n \pm 1, m \pm 1)$, the only non-zero $U_{n,m::l,k}(t)$ are such that $n-m = l-k$.

For the initial condition of interest the atom is in the upper state $|2\rangle$ and the single mode is in the vacuum state and the reservoir of continuum quasimodes in the vacuum state we have

$$\widehat{\rho}_I = \widehat{\rho}_{SI}\,\widehat{\rho}_{RI} \qquad (42)$$
$$\widehat{\rho}_{SI} = |0;2\rangle\langle0;2| \qquad (43)$$
$$\widehat{\rho}_{RI} = \prod_{\Delta}(|0\rangle\langle0|)_{\Delta}, \qquad (44)$$

and hence the only non-zero $\rho(n,m,0)$ is for $n=m=2$

$$\rho(2,2,0) = \begin{bmatrix} 1 \\ 0 \\ 0 \\ 0 \\ 0 \\ 0 \\ 0 \\ 0 \\ 0 \end{bmatrix}. \qquad (45)$$

For the discussion above regarding the irreversible linking of the coupled sets of density matrix elements, the unique solution for this initial condition is such that all $\rho(n,m,t)$ are zero except $\rho(2,2,t)$, $\rho(1,1,t)$ and $\rho(0,0,t)$, which are obtained from their Laplace transforms

$$\widetilde{\rho}(2,2,s) = (s+iA(2,2))^{-1}\,\rho(2,2,0)$$
$$\widetilde{\rho}(1,1,s) = (s+iA(1,1))^{-1}\,iB(1,1)\,\widetilde{\rho}(2,2,s)$$
$$\widetilde{\rho}(0,0,s) = (s+iA(0,0))^{-1}\,iB(0,0)\,\widetilde{\rho}(1,1,s). \qquad (46)$$

This solution involves inverting a 9×9 and a 4×4 matrix. For this case of finite initial energy, the spectrum will be be that associated with a finite photon pulse in the cavity, but as we will see the spectrum will be different to that for spontaneous emission from an excited three-level cascade atom in free space.

For the evolution matrices that are required for determining the spectra we have the solutions

$$\widetilde{U}(1,0::1,0;s) = (s+iA(1,0))^{-1}$$
$$\widetilde{U}(n+1,n::1,0;s) = 0 \qquad (n > 1), \qquad (47)$$

and

$$\widetilde{U}(2,1::2,1;s) = (s+iA(2,1))^{-1}$$
$$\widetilde{U}(1,0::2,1;s) = (s+iA(1,0))^{-1}$$
$$\times iB(1,0)\,(s+iA(2,1))^{-1}$$
$$\widetilde{U}(n+1,n::2,1;s) = 0 \qquad (n > 1). \qquad (48)$$

This solution corresponds to the previous result that an initial density matrix with only non-zero elements in the (N,M) set or below cannot evolve into a density matrix with non-zero elements in sets such as $(N+1,M+1)$, $(N+2,M+2),\dots$, due to the irreversible nature of the relaxation processes. Further details are in Appendix B.

B. Detector atom inside cavity—Case A

To evaluate the spectrum for the case where the detector atom is inside the high Q cavity ($CaseA$) and with initial conditions of the atom excited and the cavity mode empty of photons we take

$$\widehat{V}_- = \mu^*\,\widehat{a}$$
$$= \mu^*\sum_{n\nu}\sqrt{n}\,|n-1;\nu\rangle\langle n;\nu| \qquad (49)$$
$$\widehat{V}_+ = \mu\,\widehat{a}^\dagger$$
$$= \mu\sum_{m\lambda}\sqrt{m}\,|m;\lambda\rangle\langle m-1;\lambda|. \qquad (50)$$

The two time correlation function is then

$$Tr_{SR}\left(\widehat{\rho}_I\,\widehat{V}_+(t_2)\,\widehat{V}_-(t_1)\right)$$
$$= |\mu|^2\sum_{m\lambda}\sum_{n\nu}\sqrt{m}\sqrt{n}\,\left\langle \widehat{S}_{m\lambda;\overline{m-1}\lambda}(t_2)\widehat{S}_{\overline{n-1}\nu;\,n\nu}(t_1)\right\rangle, \qquad (51)$$

where the transition operators $\widehat{S}_{m\lambda;\,n\nu}(t) \equiv |m;\lambda\rangle\langle n;\nu|$ are Heisenberg operators at time t, and the trace is over both system and reservoir states. The two time correlation functions can be evaluated using the quantum regression theorem [12, 40, 41], the result for which is given in terms of the evolution operator matrix elements $U_{m\lambda;\,n\nu::l\beta;\,k\alpha}(\tau)$ associated with the density matrix equations and considered as a function of the time difference $\tau = |t_1 - t_2| \geqslant 0$, and density matrix elements

$\rho_{m\lambda;\,n\nu}(t_{1,2})$ considered as a function of the smaller of the two times t_1 and t_2. The derivation of the expression for the spectrum for Case A is given in Appendix B.

The spectrum is given by

$$S(\omega) = S_2(\omega) + S_6(\omega), \tag{52}$$

with

$$S_2(\omega) = 2\,\mathrm{Re}\,\frac{|\mu|^2}{\hbar^2}\sqrt{1}\sqrt{1}\times\{\widetilde{\rho}_{10;\,10}(\epsilon')\widetilde{U}_{10;\,00::01;\,00}(-i\omega+\epsilon) + \widetilde{\rho}_{01;\,10}(\epsilon')\widetilde{U}_{10;\,00::10;\,00}(-i\omega+\epsilon)\} \tag{53}$$

$$\begin{aligned}
S_6(\omega) = 2\,\mathrm{Re}\,\frac{|\mu|^2}{\hbar^2}\,[\,&\sqrt{1}\,\widetilde{\rho}_{02;\,11}(\epsilon')\{\sqrt{1}\widetilde{U}_{10,00::02;\,01}(-i\omega+\epsilon) + \sqrt{1}\widetilde{U}_{11,01::02;\,01}(-i\omega+\epsilon) + \sqrt{2}\widetilde{U}_{20,10::02;\,01}(-i\omega+\epsilon)\} \\
&+\sqrt{2}\,\widetilde{\rho}_{02;\,20}(\epsilon')\{\sqrt{1}\widetilde{U}_{10,00::02;\,10}(-i\omega+\epsilon) + \sqrt{1}\widetilde{U}_{11,01::02;\,10}(-i\omega+\epsilon) + \sqrt{2}\widetilde{U}_{20,10::02;\,10}(-i\omega+\epsilon)\} \\
&+\sqrt{1}\,\widetilde{\rho}_{11;\,11}(\epsilon')\{\sqrt{1}\widetilde{U}_{10,00::11;\,01}(-i\omega+\epsilon) + \sqrt{1}\widetilde{U}_{11,01::11;\,01}(-i\omega+\epsilon) + \sqrt{2}\widetilde{U}_{20,10::11,01}(-i\omega+\epsilon)\} \\
&+\sqrt{2}\,\widetilde{\rho}_{11;\,20}(\epsilon')\{\sqrt{1}\widetilde{U}_{10,00::11,10}(-i\omega+\epsilon) + \sqrt{1}\widetilde{U}_{11,01::11,10}(-i\omega+\epsilon) + \sqrt{2}\widetilde{U}_{20,10::11;\,10}(-i\omega+\epsilon)\} \\
&+\sqrt{1}\,\widetilde{\rho}_{20;\,11}(\epsilon')\{\sqrt{1}\widetilde{U}_{10,00::20;\,01}(-i\omega+\epsilon) + \sqrt{1}\widetilde{U}_{11,01::20;\,01}(-i\omega+\epsilon) + \sqrt{2}\widetilde{U}_{20,10::20;\,01}(-i\omega+\epsilon)\} \\
&+\sqrt{2}\,\widetilde{\rho}_{20;\,20}(\epsilon')\{\sqrt{1}\widetilde{U}_{10,00::20,10}(-i\omega+\epsilon) + \sqrt{1}\widetilde{U}_{11,01::20,10}(-i\omega+\epsilon) + \sqrt{2}\widetilde{U}_{20,10::20,10}(-i\omega+\epsilon)\}\,].
\end{aligned} \tag{54}$$

We see that in Case A, the spectrum involves Laplace transforms of the evolution operator from the $U_{1,0::1,0}(t)$, $U_{1,0::2,1}(t)$ and $U_{2,1::2,1}(t)$ matrices and from the $\rho(2,2,t)$ and $\rho(1,1,t)$ density matrix elements. The spectrum is calculated from the equation (52) using the results from equations (46), (47) and (48). The spectral variable ω occurs in the $\widetilde{U}$ matrices associated with $(1,0)$ and $(2,1)$ sets. From the equations determining these, it is easy to see that the spectral variable appears via the factor $\Delta\omega = (\omega - \omega_c)$, so the spectra can be shown as functions of the detuning of the spectral variable from the cavity frequency. The calculation requires inverting 6×6 and 2×2 matrices as a function of the spectral variable ω to give the $\widetilde{U}$ terms and inverting 9×9 and 4×4 matrices to give the $\widetilde{\rho}$ terms.

C. Detector atom outside cavity—Case B (end emission)

To evaluate the spectrum in the case where the detector atom is outside the cavity to detect end emission and thus samples the continuum cavity quasimodes (*Case B*) and with the same initial conditions as before we now take

$$\widehat{V}_- = \int d\Delta\,\rho_C(\Delta)\,\mu^*(\Delta)\widehat{b}(\Delta), \tag{55}$$

and will assume that $\mu^*(\Delta)$ is also a slowly varying function of Δ.

Starting from the formal solutions of Heisenberg equations of motion for the Heisenberg operators $\widehat{b}(\Delta, t)$ and $\widehat{a}(t)$ and making a Markoff approximation based on slowly varying factors $\rho_C(\Delta)$, $\mu^*(\Delta)$ and $W^*(\Delta)$, we can show that $\widehat{V}_-$ is the sum of a free field term $\widehat{V}_-^F$ and a cavity term $\widehat{V}_-^C$, where

$$\widehat{V}_- = \widehat{V}_-^F + \widehat{V}_-^C \tag{56}$$

$$\widehat{V}_-^F = \int d\Delta\,\rho_C(\Delta)\,\mu^*(\Delta)\,\exp(-i\Delta t)\,\widehat{b}(\Delta) \tag{57}$$

$$\widehat{V}_-^C = M^*\widehat{a}, \tag{58}$$

and where

$$M^* = \int d\Delta\,\frac{\rho_C(\Delta)\,\mu^*(\Delta)\,W^*(\Delta)}{\omega_c - \Delta + i\epsilon} \tag{59}$$

is an effective dipole coupling constant. Thus the cavity contribution $\widehat{V}_-^C$ to the spectral quantity $\widehat{V}_-$ is the same as for Case A, apart from a constant of proportionality. The details are given in Appendix C.

The expression for the two-time correlation function will involve free evolution continuum quasimode contributions of the form $Tr_{SR}\left(\widehat{\rho}_I\,\widehat{V}_+^F(t_2)\,\widehat{V}_-^F(t_1)\right)$, cross terms involving the continuum and cavity quasimode contributions of the form $Tr_{SR}\left(\widehat{\rho}_I\,\widehat{V}_+^F(t_2)\,\widehat{V}_-^C(t_1)\right), Tr_{SR}\left(\widehat{\rho}_I\,\widehat{V}_+^C(t_2)\,\widehat{V}_-^F(t_1)\right)$ and purely cavity quasimode contributions of the

form $Tr_{SR}\left(\widehat{\rho}_I\,\widehat{V}_+^C(t_2)\,\widehat{V}_-^C(t_1)\right)$. Since the continuum quasimodes are in the vacuum state it is not difficult to see using results such as $\widehat{b}(\Delta)(|0\rangle\langle0|)_\Delta = 0$ and $(|0\rangle\langle0|)_\Delta\widehat{b}^\dagger(\Delta) = 0$, that the continuum quasimode term and the two cross terms all give zero, leaving behind only the cavity quasimode contribution

$$Tr_{SR}\left(\widehat{\rho}_I\,\widehat{V}_+(t_2)\,\widehat{V}_-(t_1)\right) = Tr_{SR}\left(\widehat{\rho}_I\,\widehat{V}_+^C(t_2)\,\widehat{V}_-^C(t_1)\right),\tag{60}$$

where

$$\widehat{V}_-^C = M^*\sum_{n\nu}\sqrt{n}\,|n-1;\nu\rangle\langle n;\nu|\tag{61}$$

$$\widehat{V}_+^C = M\sum_{m\lambda}\sqrt{m}\,|m;\lambda\rangle\langle m-1;\lambda|.\tag{62}$$

The spectrum for Case B will therefore have the same form as that for Case A.

D. Detector atom outside cavity—Case C (side emission)

In the case where the detector atom is outside the cavity to detect side emission, and thus responds to the atomic transition operators (*Case C*), we have

$$\widehat{V}_- = R_2^*\,\widehat{\sigma}_2^- + R_1^*\,\widehat{\sigma}_1^-\tag{63}$$

$$= R_2^*\sum_n|n;1\rangle\langle n;2| + R_1^*\sum_n|n;0\rangle\langle n;1|\tag{64}$$

$$\widehat{V}_+ = R_2\,\widehat{\sigma}_2^+ + R_1\,\widehat{\sigma}_1^+\tag{65}$$

$$= R_2\sum_m|m;2\rangle\langle m;1| + R_1\sum_m|m;1\rangle\langle m;0|\tag{66}$$

where we have used the notation $R_{12}\to R_2$, $R_{01}\to R_1$. Since both R_2 and g_2 are both proportional to the scalar product of the vector dipole matrix element $\langle2|\,\overrightarrow{\widehat{d}}\,|1\rangle$ between the upper and intermediate state with either the polarization unit vector for the spontaneous emission modes or the cavity quasimode, and similarly for R_1 and g_1 in regard to the vector dipole matrix element $\langle1|\,\overrightarrow{\widehat{d}}\,|0\rangle$ between the intermediate and lower state, it follows that

$$\frac{R_2}{R_1} = \frac{g_2}{g_1}.\tag{67}$$

Since we have chosen g_1 and g_2 to be real we will make the same choice for R_1 and R_2 from now on.

Hence the two-time correlation function is

$$
\begin{aligned}
&Tr_{SR}\left(\widehat{\rho}_I\,\widehat{V}_+(t_2)\,\widehat{V}_-(t_1)\right)\\
&= R_2^2\sum_m\sum_n\left\langle\widehat{S}_{m2;\,m1}(t_2)\widehat{S}_{n1;\,n2}(t_1)\right\rangle\\
&\quad+R_1^2\sum_m\sum_n\left\langle\widehat{S}_{m1;\,m0}(t_2)\widehat{S}_{n0;\,n1}(t_1)\right\rangle\\
&\quad+R_2R_1\sum_m\sum_n\left\langle\widehat{S}_{m2;\,m1}(t_2)\widehat{S}_{n0;\,n1}(t_1)\right\rangle\\
&\quad+R_1R_2\sum_m\sum_n\left\langle\widehat{S}_{m1;\,m0}(t_2)\widehat{S}_{n1;\,n2}(t_1)\right\rangle.
\end{aligned}\tag{68}
$$

Note the four contributions to the spectrum, two involve just one atomic transition, the other two involve both transitions. The possibility of interference terms is clear. The derivation of the expression for the spectrum is given in Appendix D

The spectrum is given by

$$
\begin{aligned}
S(\omega) = {}&2\,\mathrm{Re}\,\frac{R_2^2}{\hbar^2}[\ \ \widetilde{U}_{02;\,01::20;\,01}(-i\omega+\epsilon)\,\widetilde{\rho}_{20;\,02}(\epsilon') + \widetilde{U}_{02;\,01::11;\,01}(-i\omega+\epsilon)\,\widetilde{\rho}_{11;\,02}(\epsilon')\\
&\qquad+\widetilde{U}_{02;\,01::02;\,01}(-i\omega+\epsilon)\,\widetilde{\rho}_{02;\,02}(\epsilon')]\\
&+2\,\mathrm{Re}\,\frac{R_1^2}{\hbar^2}[\ \ \widetilde{U}_{01;\,00::01;\,00}(-i\omega+\epsilon)\,\widetilde{\rho}_{01;\,01}(\epsilon') + \widetilde{U}_{01;\,00::10;\,00}(-i\omega+\epsilon)\,\widetilde{\rho}_{10;\,01}(\epsilon')\\
&\qquad+\{\widetilde{U}_{01;\,00::02;\,10}(-i\omega+\epsilon)\ +\ \widetilde{U}_{11;\,10::02;\,10}(-i\omega+\epsilon)\}\,\widetilde{\rho}_{02;\,11}(\epsilon')\\
&\qquad+\{\widetilde{U}_{01;\,00::11;\,10}(-i\omega+\epsilon) + \widetilde{U}_{11;\,10::11;\,10}(-i\omega+\epsilon)\}\,\widetilde{\rho}_{11;\,11}(\epsilon')\\
&\qquad+\{\widetilde{U}_{01;\,00::20;\,10}(-i\omega+\epsilon) + \widetilde{U}_{11;\,10::20;\,10}(-i\omega+\epsilon)\}\,\widetilde{\rho}_{20;\,11}(\epsilon')]\\
&+2\,\mathrm{Re}\,\frac{R_2R_1}{\hbar^2}[\ \ \{\widetilde{U}_{01;\,00::02;\,01}(-i\omega+\epsilon) + \widetilde{U}_{11;\,10::02;\,01}(-i\omega+\epsilon)\}\,\widetilde{\rho}_{02;\,02}(\epsilon')\\
&\qquad+\{\widetilde{U}_{01;\,00::11;\,01}(-i\omega+\epsilon) + \widetilde{U}_{11;\,10::11;\,01}(-i\omega+\epsilon)\}\,\widetilde{\rho}_{11;\,02}(\epsilon')\\
&\qquad+\{\widetilde{U}_{01;\,00::20;\,01}(-i\omega+\epsilon) + \widetilde{U}_{11;\,10::20;\,01}(-i\omega+\epsilon)\}\,\widetilde{\rho}_{20;\,02}(\epsilon')]\\
&+2\,\mathrm{Re}\,\frac{R_1R_2}{\hbar^2}[\ \ \widetilde{U}_{02;\,01::02;\,10}(-i\omega+\epsilon)\,\widetilde{\rho}_{02;\,11}(\epsilon') + \widetilde{U}_{02;\,01::11;\,10}(-i\omega+\epsilon)\,\widetilde{\rho}_{11;\,11}(\epsilon')\\
&\qquad+\widetilde{U}_{02;\,01::20;\,10}(-i\omega+\epsilon)\,\widetilde{\rho}_{20;\,11}(\epsilon')].
\end{aligned}\tag{69}
$$

We see that as in Case A (and Case B), the spectrum involves Laplace transforms of the evolution operator from

the $U_{1,0::2,1}(t)$, $U_{2,1::2,1}(t)$ and $U_{1,0::1,0}(t)$, and from the density matrix elements $\rho(2,2,t)$ and $\rho(1,1,t)$. However, in Case C different elements are involved, so although the spectra will be qualitatively similar in the two cases there will be quantitative differences. The spectrum is calculated from the equation (69) using the results from equations (46), (47) and (48). The spectral variable ω occurs in the $\widetilde{U}$ matrices associated with $(1,0)$ and $(2,1)$ sets. From the equations determining these, it is easy to see that the spectral variable appears via the factor $\Delta\omega = (\omega - \omega_c)$, so again the spectra can be shown as functions of the detuning of the spectral variable from the cavity frequency.

IV. CASCADE ATOM SPECTRUM: NUMERICAL RESULTS

Results for the spontaneous emission spectra from the three level cascade atom in a damped high-Q cavity are presented in figures 3–11 and figures 13–14. In all cases the spectrum $S(\omega)$ is shown as a function of the detuning $\Delta\omega = \omega - \omega_c$ of the spectral variable ω from the cavity frequency ω_c. A logarithmic scale is used for $S(\omega)$ in order to highlight the numerous spectral peaks, and $\Delta\omega$ is in units of $g = g_2$. The spectrum for Case A(B)—detector in cavity or end emission—is calculated from equation (52) and the spectrum for Case C—side emission is calculated from equation (69). In all cases, except figures 13 and 14, the values of the coupling constants are $g_1 = g_2 = 1.0$ for numerical computation. For Case A(B) the detector atom-cavity mode coupling constant is $\mu = 1.0$ ($M = 1.0$), whilst for Case C the detector atom-cascade atom coupling constants are $R_1 = R_2 = 1.0$ (except in figures 13 and 14). The spectra are shown for various choices of the cavity detuning δ, the half difference between the two atomic transition frequencies $\overline{\delta}$, and the cavity decay rate Γ. Strong coupling cases $g \gg \Gamma$ and intermediate coupling cases $g \sim \Gamma$ are displayed in the figures.

Spectral calculations can also be based on a derivation of the spectra using density matrix elements defined in terms of dressed atom states, rather than the uncoupled states that we have used here. This can result in simpler expressions in the strong coupling regime, where line width factors are small compared to dressed atom level splittings. Analytical formulae for positions, heights and widths of spectral peaks can be often obtained in the strong coupling regime. However, for calculations covering the weak, intermediate and strong coupling regimes using the dressed atom basis does not gain much advantage and for the present the uncoupled basis will be used.

Figure 3 is for the case of resonance, with $\overline{\delta} = \delta = 0.0$, where the two atomic transition frequencies are equal and the same as the cavity frequency. A strong coupling situation with $\Gamma = 0.1$ is presented for both Case A(B) and Case C. A symmetrical six peak spectrum is shown. For Case C the spectral intensity becomes very small
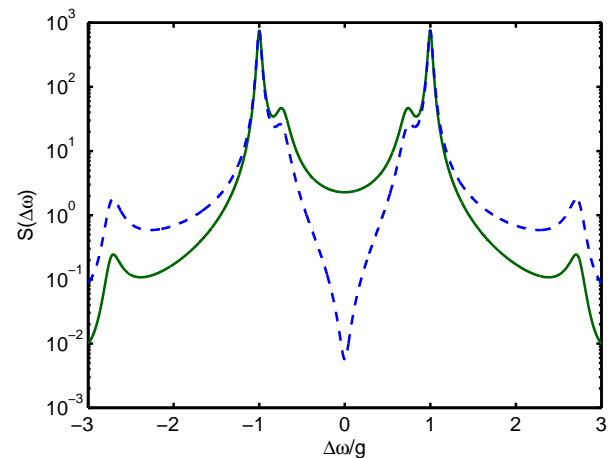

FIG. 3: Cascade atom in high-Q cavity. SE spectra $S(\omega)$ versus spectral detuning from cavity frequency $\Delta\omega = (\omega - \omega_c)$. The case of resonance is shown, where each transition is resonant with the cavity frequency, $\delta = \overline{\delta} = 0$. The coupling constants are $g_1 = g_2 = 1$ and the detector coupling constants are $\mu = R_1 = R_2 = 1$. The cavity decay is $\Gamma = 0.1$. The solid line is for Case A(B)—end emission—and the dashed line is for Case C—side emission.

when the spectral frequency equals the cavity frequency, i.e. when $\Delta\omega = 0$. This effect is not seen for Case A(B) and indicates the presence of interference effects.

Figures 4 and 5 are also for the same resonance situation as in figure 3, $\overline{\delta} = \delta = 0.0$ for Case A(B) and Case C respectively. In these figures the cavity decay rate Γ takes on the values $\Gamma = 1.0$, 0.1 and 0.01, traversing the regime from intermediate coupling to very strong coupling. In the strong and very strong coupling cases $\Gamma = 0.1$ and 0.01 the six peaks are very clearly seen, whilst for intermediate coupling only two peaks remain due to the line broadening effect of the larger cavity decay. Again, for Case C (figure 5) the spectral intensity tends to zero for $\Delta\omega = 0$ and $\Gamma = 0.1$ and 0.01. However, for $\Gamma = 1.0$, the spectral hole is suppressed and in fact the spectrum in Case C is very similar to that of Cases A(B) for $\Gamma = 1.0$ as seen in figure 4. We know that for a two-level system in the low-Q limit the cavity field operators can be adiabatically eliminated in favour of the atomic operators, i.e. the cavity field 'follows' the atomic state. For this reason we might expect that spectra based on field operators (case A) and spectra based on the atomic operators (case C) would become similar in this limit.

Figures 6 and 7 for Cases A(B) and Case C respectively, apply to the situation where the two atomic transition frequencies are the same $\overline{\delta} = 0.0$, but where the cavity detuning δ may be non-zero. Cases where $\delta = 0.0$ (resonance), -1.0 and -2.0 are shown. A strong coupling situation with $\Gamma = 0.1$ applies in both figures. The effect of cavity detuning is that the six peak symmetrical spectra, applying for resonance, are replaced by asymmetrical spectra still with six peaks, but with the hint that other peaks may be hidden in the relatively broad
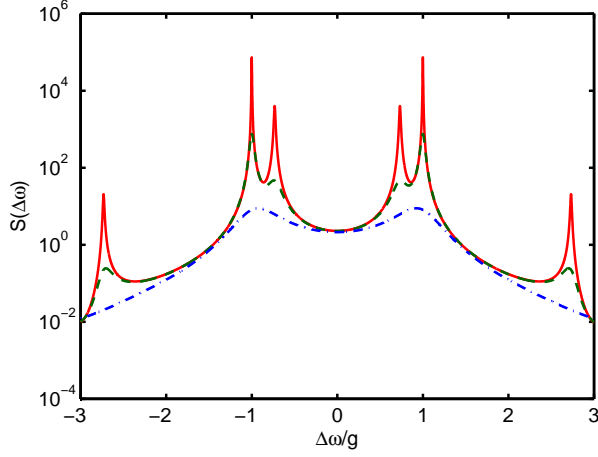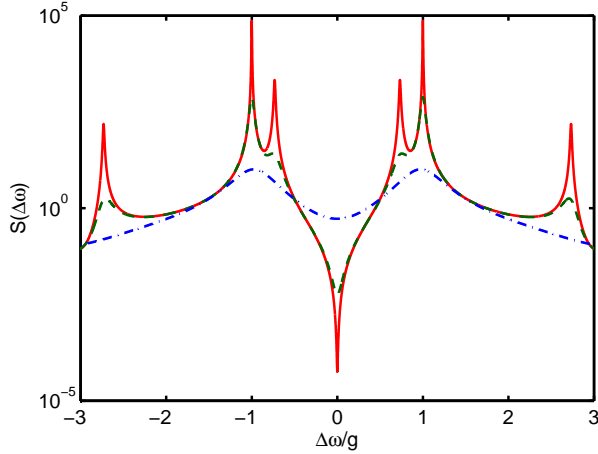
13

FIG. 4: Cascade atom in high-Q cavity. SE spectra $S(\omega)$ versus spectral detuning from cavity frequency $\Delta\omega = (\omega - \omega_c)$. The case of resonance is shown, where each transition is resonant with the cavity frequency, $\delta = \bar{\delta} = 0$. The coupling constants are $g_1 = g_2 = 1$ and the detector coupling constant is $\mu = 1$. The cavity decay $\Gamma = 0.01$ is the solid line, $\Gamma = 0.1$ is the dashed line and $\Gamma = 1.0$ is the chained line. The spectrum for Case A(B)—end emission—is shown.

FIG. 5: Cascade atom in high-Q cavity. SE spectra $S(\omega)$ versus spectral detuning from cavity frequency $\Delta\omega = (\omega - \omega_c)$. The case of resonance is shown, where each transition is resonant with the cavity frequency, $\delta = \bar{\delta} = 0$. The coupling constants are $g_1 = g_2 = 1$ and the detector coupling constants are $R_1 = R_2 = 1$. The cavity decay $\Gamma = 0.01$ is the solid line, $\Gamma = 0.1$ is the dashed line and $\Gamma = 1.0$ is the chained line. The spectrum for Case C—side emission—is shown.

features. Again the hole in the intensity for Case C near $\Delta\omega = 0$ remains when the detuning is non-zero, though it is not as deep as in figure 5 for $\Gamma = 0.1$ (dashed curve).

Figures 8 and 9 for Cases A(B) and Case C respectively, also apply to the situation where the two atomic transition frequencies are the same, $\bar{\delta} = 0.0$, but where the cavity detuning δ may be non-zero. Now a very strong coupling situation with $\Gamma = 0.01$ applies in both
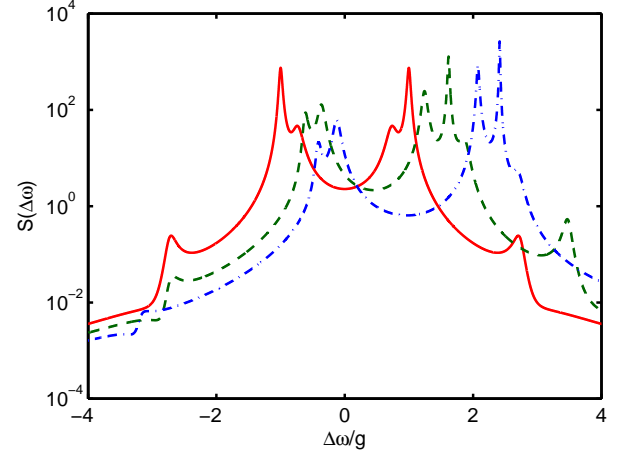

FIG. 6: Cascade atom in high-Q cavity. SE spectra $S(\omega)$ versus spectral detuning from cavity frequency $\Delta\omega = (\omega - \omega_c)$. The case of equal atomic transition frequencies is shown, but with the cavity frequency is detuned from the average of the two transition frequencies. $\bar{\delta} = 0$ but δ may be non-zero. The coupling constants are $g_1 = g_2 = 1$ and the detector coupling constant is $\mu = 1$. The cavity decay is $\Gamma = 0.1$. The cavity detuning $\delta = 0$ is the solid line, $\delta = -1$ is the dashed line, $\delta = -2$ is the chained line. The spectrum for Case A(B)—end emission—is shown.
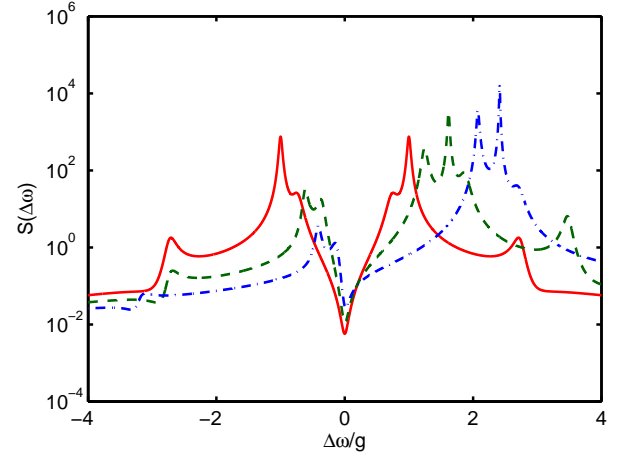

FIG. 7: Cascade atom in high-Q cavity. SE spectra $S(\omega)$ versus spectral detuning from cavity frequency $\Delta\omega = (\omega - \omega_c)$. The case of equal atomic transition frequencies is shown, but with the cavity frequency is detuned from the average of the two transition frequencies. $\bar{\delta} = 0$, but δ may be non-zero. The coupling constants are $g_1 = g_2 = 1$ and the detector coupling constants are $R_1 = R_2 = 1$. The cavity decay is $\Gamma = 0.1$. The cavity detuning $\delta = 0$ is the solid line, $\delta = -1$ is the dashed line, $\delta = -2$ is the chained line. The spectrum for Case C—side emission—is shown.

figures, so that the spectral peaks will become narrower. Cases where $\delta = 0.0$ (resonance) and -1.0 are shown. It is now clearly shown that the effect of detuning is to replace the six peak symmetrical spectrum for the resonance case, with eight peaks. We also note that in
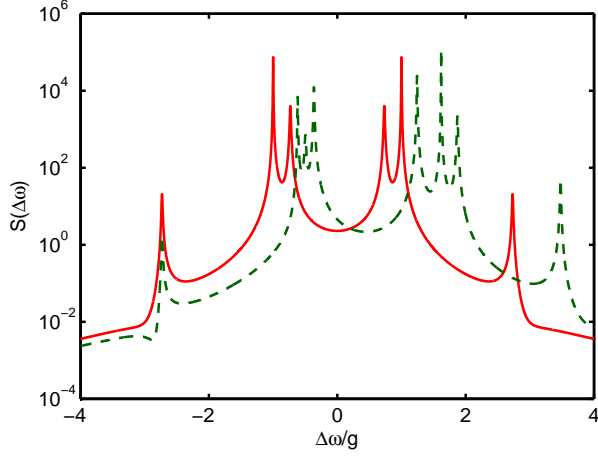
FIG. 8: Cascade atom in high-Q cavity. SE spectra $S(\omega)$ versus spectral detuning from cavity frequency $\Delta\omega = (\omega - \omega_c)$. The case of equal atomic transition frequencies is shown, but with the cavity frequency is detuned from the average of the two transition frequencies. $\bar{\bar{\delta}} = 0$, but δ may be non-zero. The coupling constants are $g_1 = g_2 = 1$ and the detector coupling constant is $\mu = 1$. The cavity decay is $\Gamma = 0.01$. The cavity detuning $\delta = 0$ is the solid line, $\delta = -1$ is the dashed line. The spectrum for Case A(B)—end emission—is shown.
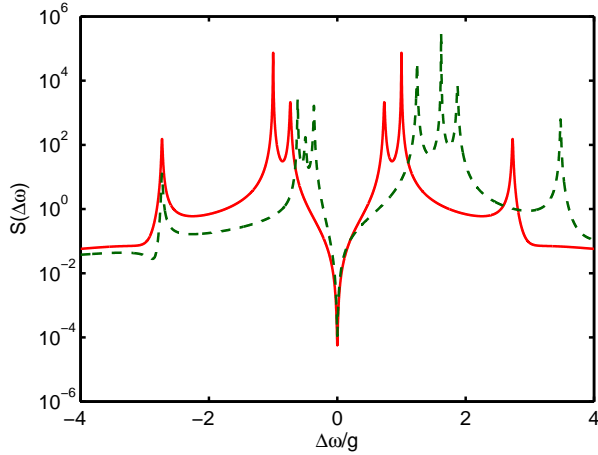

FIG. 9: Cascade atom in high-Q cavity. SE spectra $S(\omega)$ versus spectral detuning from cavity frequency $\Delta\omega = (\omega - \omega_c)$. The case of equal atomic transition frequencies is shown, but with the cavity frequency is detuned from the average of the two transition frequencies. $\bar{\bar{\delta}} = 0$, but δ may be non-zero. The coupling constants are $g_1 = g_2 = 1$ and the detector coupling constants are $R_1 = R_2 = 1$. The cavity decay is $\Gamma = 0.01$. The cavity detuning $\delta = 0$ is the solid line, $\delta = -1$ is the dashed line. The spectrum for Case C—side emission—is shown.

the detuned case one of the peaks displays a distinctly dispersion-like line shape. The spectral hole at $\Delta\omega = 0$ for Case C now reaches an even lower intensity (10^{-4} units) than for figure 7 (10^{-2} units), and is equally sharp for the detuned case as for resonance.
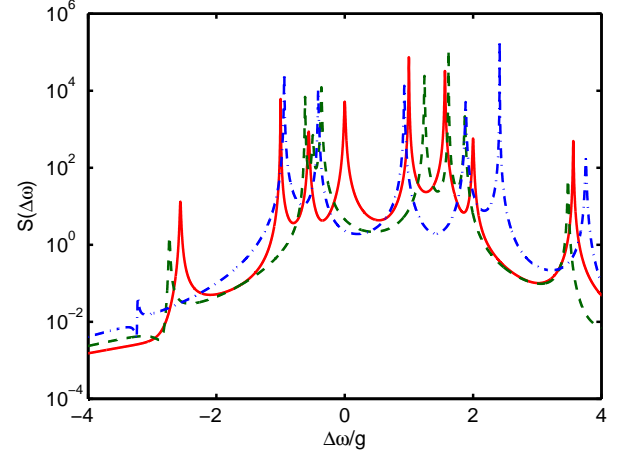

FIG. 10: Cascade atom in high-Q cavity. SE spectra $S(\omega)$ versus spectral detuning from cavity frequency $\Delta\omega = (\omega - \omega_c)$. The case of cavity detuning from the average of the two transition frequencies $\delta = -1$. The atomic transition frequencies may be different. The coupling constants are $g_1 = g_2 = 1$ and the detector coupling constant is $\mu = 1$. The cavity decay is $\Gamma = 0.01$. The half atomic transition frequency difference $\bar{\bar{\delta}} = -1 = +\delta$ is the solid line, $\bar{\bar{\delta}} = 0$ is the dashed line and $\bar{\bar{\delta}} = 1 = -\delta$ is the chained line. For $\bar{\bar{\delta}} = +\delta, -\delta$ the cavity frequency coincides with the lower, upper atomic transition frequency respectively. The spectrum for Case A(B)—end emission—is shown.
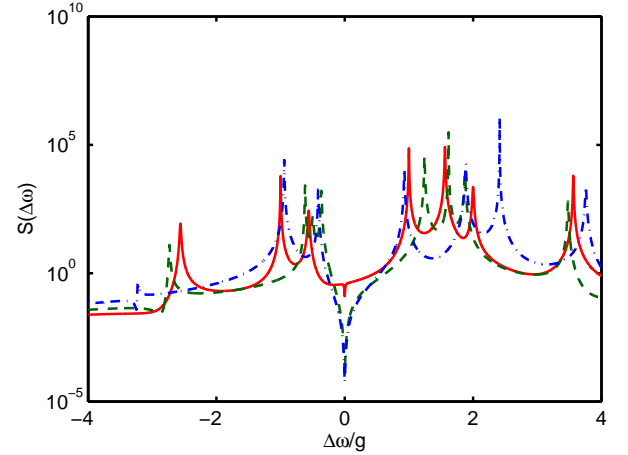

FIG. 11: Cascade atom in high-Q cavity. SE spectra $S(\omega)$ versus spectral detuning from cavity frequency $\Delta\omega = (\omega - \omega_c)$. The case of cavity detuning from the average of the two transition frequencies $\delta = -1$. The atomic transition frequencies may be different. The coupling constants are $g_1 = g_2 = 1$ and the detector coupling constants are $R_1 = R_2 = 1$. The cavity decay is $\Gamma = 0.01$. The half atomic transition frequency difference $\bar{\bar{\delta}} = -1 = +\delta$ is the solid line, $\bar{\bar{\delta}} = 0$ is the dashed line and $\bar{\bar{\delta}} = 1 = -\delta$ is the chained line. For $\bar{\bar{\delta}} = +\delta, -\delta$ the cavity frequency coincides with the lower, upper atomic transition frequency respectively. The spectrum for Case C—side emission—is shown.

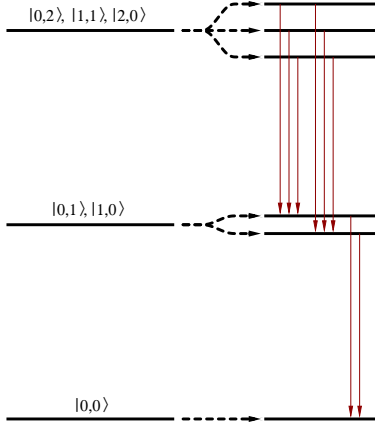Figures 10 and 11 for Cases A(B) and Case C respec-

FIG. 12: The uncoupled atom-cavity mode energy levels and the dressed atom energy levels allowing for atom-cavity mode coupling. The situation shown is that of resonance and with equidistant cascade atom levels. $\delta = \overline{\delta} = 0$. The uncoupled states are denoted $|n;\nu\rangle$, where $n = 0,1,2,\ldots$ gives the number of photons in the cavity mode and $\nu = 0,1,2$ lists the cascade atom states. The three lowest dressed atom multiplets (singlet, doublet, triplet) are shown. Allowed transitions between the dressed atom states are indicated.

tively, apply to the situation where the cavity frequency is detuned from the average of the atomic transition frequencies, and where these atomic transition frequencies may themselves be different. The cavity detuning is $\delta = -1.0$ in both figures. A very strong coupling situation with $\Gamma = 0.01$ applies in both figures so that the spectral peaks will become narrower. Cases where $\overline{\delta} = -1.0 = +\delta$, $\overline{\delta} = 0.0$ (both atomic transition frequencies equal) and $\overline{\delta} = +1.0 = -\delta$ are shown. Note that for the case $\overline{\delta} = -\delta$, the cavity frequency coincides with the upper atomic transition frequency ($\omega_c = \omega_1$), whilst the case $\overline{\delta} = +\delta$, the cavity frequency coincides with the lower atomic transition frequency ($\omega_c = \omega_2$). In both Case A(B) and Case C up to eight spectral peaks occur. For Case C (see figure 11) an interesting feature is that the spectral hole at $\Delta\omega = 0$ is not present when the cavity frequency is resonant with the lower atomic transition frequency ($\overline{\delta} = +\delta$), but is still present when the cavity frequency is resonant with the upper atomic transition frequency.

The same general features for the present Case A(B) and Case C situation in terms of the numbers of spectral features were found by Zhou et al. [28], but the presence of the spectral hole at $\Delta\omega = 0$ for Case C (which they referred to as the emission spectrum) and its relationship to quantum interference was not reported in their paper. Their lineshapes were associated only with the finite spectrometer bandwidth incorporated in their definition of the spectra and did not reflect cavity decay—which was assumed to be zero.

The spectral features can be interpreted in terms of the dressed atom model [7]. Figure 12 shows the uncoupled atom-cavity mode states and their splitting into dressed

atom states for the three lowest dressed atom multiplets in the case of resonance $\delta = \overline{\delta} = 0$. The lowest multiplet is a singlet and is based on the $|0;0\rangle$ uncoupled states. The next lowest multiplet is a doublet and is based on the $|0;1\rangle$ and $|1;0\rangle$ uncoupled states. The next lowest multiplet is a triplet and is based on the $|0;2\rangle$, $|1;1\rangle$ and $|2;0\rangle$ uncoupled states. These are of course the only states that could be occupied in the cascade atom decay process. The uncoupled levels are separated by an energy $\hbar\omega_c = \hbar\omega_0$. For the resonance case the averages of dressed atom multiplet levels does not change from the uncoupled energies, and the triplet levels are equispaced. For the resonance case, the energies of the three triplet states relative to the uncoupled energy are $+\hbar\sqrt{2g_1^2 + g_2^2}$, 0, $-\hbar\sqrt{2g_1^2 + g_2^2}$, whilst those for the doublet state are $+\hbar g_1$, $-\hbar g_1$ and 0 for the singlet state. The position for the spectral features is in accord with these dressed atom energies. For non-zero δ, $\overline{\delta}$ the dressed atom multiplets do not have these symmetry features. The selection rules for electric dipole processes only allow transitions between neighbouring dressed atom multiplets. It is therefore easy to see from figure 12 that there will be up to eight different possible transition frequencies, all clustered around $\omega = \omega_c$, and in non-zero δ, $\overline{\delta}$ situations all eight frequencies could be present. In the resonance case $\delta = \overline{\delta} = 0$ the symmetry feature results in the middle to bottom dressed atom transition frequencies coinciding with two of the upper to middle dressed atom transition frequencies, thereby reducing the number of distinct lines to six in this case. The fact that photons of the same frequency could have come from either an upper to middle or a middle to lower dressed atom transition, and that these processes cannot be separately measured, is likely to result in quantum interference effects.

To demonstrate the role of both upper to middle and middle to lower dressed atom transitions in the interference process, figures 13, and 14 show the effect for the resonance case of switching off the middle to lower dressed atom transitions. The figures show the spectrum for Case A(B)—end emission—as the solid lines and for Case C—side emission—as dashed lines. In these two figures the two atomic transition frequencies are equal and the same as the cavity frequency $\overline{\delta} = \delta = 0.0$, the cavity decay rate is $\Gamma = 0.01$, the value of the upper transition coupling constant is $g_2 = 1.0 = g$. For Case A(B) the detector atom-cavity mode coupling constant is $\mu = 1.0$ ($M = 1.0$), whilst for Case C the detector atom-cascade atom upper transition coupling constant is $R_2 = 1.0$. In figure 13 the lower transition and detector atom coupling constants are $g_1 = R_1 = 0.1$, for figure 14 the values are $g_1 = R_1 = 0.01$. The solid lines in previous figures 4 (Case A(B)) and 5 (Case C) show the spectra for the resonance case with $g_1 = R_1 = 1.0$, where the lower transition and detector atom coupling constants are the same as those for the upper transition. The interference hole at $\Delta\omega = 0$ for Case C is present in figure 5 is much less prominent in figure 13 and has disappeared in figure 14, as the lower dressed atom transitions have been
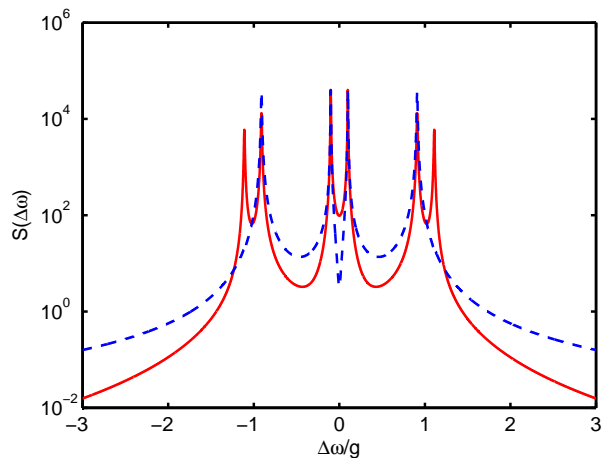
FIG. 13: Cascade atom in high-Q cavity. SE spectra $S(\omega)$ versus spectral detuning from cavity frequency $\Delta\omega = (\omega - \omega_c)$. The case of resonance is shown, where each transition is resonant with the cavity frequency, $\delta = \bar{\delta} = 0$. The coupling constants are $g_1 = 0.1$, $g_2 = 1$ and the detector coupling constants are $R_1 = 0.1$, $R_2 = 1$. The cavity decay is $\Gamma = 0.01$. The spectrum for Case A(B)—end emission—is shown as the solid line, that for Case C—side emission—is shown as the dashed line.
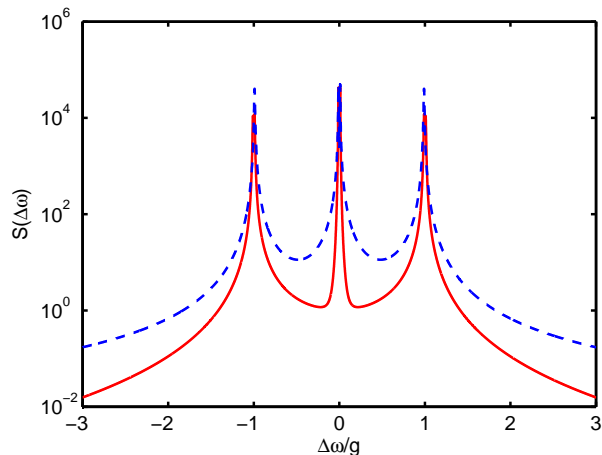

FIG. 14: Cascade atom in high-Q cavity. SE spectra $S(\omega)$ versus spectral detuning from cavity frequency $\Delta\omega = (\omega - \omega_c)$. The case of resonance is shown, where each transition is resonant with the cavity frequency, $\delta = \bar{\delta} = 0$. The coupling constants are $g_1 = 0.01$, $g_2 = 1$ and the detector coupling constants are $R_1 = 0.01$, $R_2 = 1$. The cavity decay is $\Gamma = 0.01$. The spectrum for Case A(B)—end emission—is shown as the solid line, that for Case C—side emission—is shown as the dashed line.

essentially switched off. In fact there is now a spectral peak at $\Delta\omega = 0$ for both Cases A(B) and C for the situation in figure 14. This shows that both upper to middle and middle to lower dressed atom transitions are needed to produce the destructive interference effect associated with the spectral hole.

The situation when the cavity frequency is resonant with the lower atomic transition frequency and significantly detuned from the upper atomic transition frequency is associated with a dressed atom level scheme in which the upper triplet is replaced by a doublet associated with the splitting of the degenerate uncoupled states $|1;1\rangle$ and $|2;0\rangle$ together with a separate dressed atom state which is essentially $|0;2\rangle$. The doublet based on the $|0;1\rangle$ and $|1;0\rangle$ uncoupled states is still present, as is the singlet based on $|0;0\rangle$. In this situation for Case C (side emission), the spectral hole at $\Delta\omega = 0$ is absent. For the situation when the cavity frequency is resonant with the upper atomic transition frequency and significantly detuned from the lower atomic transition frequency is associated with a dressed atom level scheme in which the upper triplet is replaced by a doublet associated with the splitting of the degenerate uncoupled states $|1;1\rangle$ and $|0;2\rangle$ together with a separate dressed atom state which is essentially $|2;0\rangle$. The doublet based on the $|0;1\rangle$ and $|1;0\rangle$ uncoupled states is now replaced by two singlets, each associated with these uncoupled states. The singlet based on $|0;0\rangle$ is unchanged. In this situation for Case C (side emission), the spectral hole at $\Delta\omega = 0$ is prominent. Why this is the case and what accounts for the general absence of the spectral hole at $\Delta\omega = 0$ for the Case A(B) (end emission) and its usual occurrence in Case C (side emission) spectra is not yet clear and a more extensive analysis is needed to find the answer, possibly based on dressed atom states. For the strong coupling regime, the use of dressed atom states may enable transition amplitudes for different processes—beginning with the same initial state with the atom in the upper state $|2\rangle$, no photons present in any mode and the detector in state $|A\rangle$ and ending in specific final states with the detector in state $|B\rangle$, to be evaluated analytically using a perturbative approach for the weak detector atom and cavity decay transitions, but treating the strong coupling processes involving the coupling constants g_1, g_2 without such an approximation. Having analytic expressions for the various quantum pathways would facilitate an understanding of the interference effects that emerge in the spectra calculated numerically via the master equation–quantum regression theorem approach.

V. CONCLUSION

In this paper we have examined the spontaneous emission spectrum from a cascade atom located inside a cavity. That spectrum was examined for three different physical situations regarding the location of an idealised detector atom. In case A the detector atom was located inside the cavity and directly influenced by the cavity field. In case B the detector atom was exposed to the field emerging from a partially transmitting cavity mirror. In case C the detector atom responded to sideways emission from the cascade atom inside the cavity. The cascade atom was initially in its uppermost level and the cavity mode empty of photons, and thus a system with

two basic excitations was studied. The spectrum was found from the weakly coupled detector atom response and involved in each case Laplace transforms of the density matrix and matrix elements of the evolution operator in a super-operator form. The spectral line-shapes only reflect cavity decay, since the weakly coupled detector atom spectrometer had zero bandwidth. Spectra have been presented for intermediate and strong coupling regime situations where both atomic transitions are resonant with the cavity frequency, for cases of non-zero cavity detuning and for cases where the two atomic transition frequencies differ.

The spectra for Case A and Case B were found to be essentially the same. The spectral features for Cases B(A) and C were qualitatively similar, with six spectral peaks for resonance cases and eight for detuned cases. These general features of the spectra could be explained via the dressed atom model. However, Case B(A) and Case C spectra differed in detail. In particular, the spectra for Case C exhibited a deep spectral hole when the spectral frequency was equal to the cavity mode frequency, a feature that persisted, for strong coupling, over a wide range of detuning and coupling conditions. However, this spectral hole was absent for Case A, a feature that cannot yet be explained. The spectral hole in Case C was particularly prominent for resonance conditions, when both atomic transition frequencies were the same and resonant with the cavity frequency. In this resonance situation, photons associated with the middle to bottom dressed atom transitions coincide in frequency with photons associated with two of the upper to middle dressed atom transitions, and therefore the origin of a photon detected in the spectrometer cannot be identified. This suggests that an interference effect is occuring, and this is confirmed by showing that the hole disappears when only the upper to middle dressed atom transitions are present. However, why the interference hole is absent

in Case B(A) spectra is still unclear. One clue is that the spectral hole in Case C spectra disappeared in figure 11 when the atomic transition frequencies were quite different and the cavity frequency was resonant with the lower atomic transition frequency. This disappearance was sensitive to both the detunings having opposite sign and a magnitude close to $g = g_1 = g_2$. The explanation is expected to be found from an examination of the dressed states in the strong coupling limit. This analysis is currently being undertaken.

APPENDIX A: COUPLED DENSITY MATRIX SETS

For the (n, m) set $(n, m \geqslant 2)$ we define the 1×9 column matrix $\rho(n, m)$ of density matrix elements in the (n, m) set as

$$\rho(n, m) = \begin{bmatrix} \rho_{\overline{n-2}2; \, \overline{m-2}2} \\ \rho_{\overline{n-2}2; \, \overline{m-1}1} \\ \rho_{\overline{n-2}2; \, m0} \\ \rho_{\overline{n-1}1; \, \overline{m-2}2} \\ \rho_{\overline{n-1}1; \, \overline{m-1}1} \\ \rho_{\overline{n-1}1; \, m0} \\ \rho_{n0; \, \overline{m-2}2} \\ \rho_{n0; \, \overline{m-1}1} \\ \rho_{n0; \, m0} \end{bmatrix}, \tag{A1}$$

and introduce suitable 9×9 matrices $A(n, m), B(n, m)$ to incorporate the couplings, detunings and decay terms

$$A(n, m) = \omega_c(n - m) \begin{bmatrix} 1&0&0&0&0&0&0&0&0 \\ 0&1&0&0&0&0&0&0&0 \\ 0&0&1&0&0&0&0&0&0 \\ 0&0&0&1&0&0&0&0&0 \\ 0&0&0&0&1&0&0&0&0 \\ 0&0&0&0&0&1&0&0&0 \\ 0&0&0&0&0&0&1&0&0 \\ 0&0&0&0&0&0&0&1&0 \\ 0&0&0&0&0&0&0&0&1 \end{bmatrix}$$

$$+ \begin{bmatrix} -\frac{1}{2}i\Gamma(p-4) & -g_2\sqrt{m-1} & 0 & g_2\sqrt{n-1} & 0 & 0 & 0 & 0 & 0 \\ -g_2\sqrt{m-1} & -(\delta+\overline{\delta})-\frac{1}{2}i\Gamma(p-3) & -g_1\sqrt{m} & 0 & g_2\sqrt{n-1} & 0 & 0 & 0 & 0 \\ 0 & -g_1\sqrt{m} & -2\delta-\frac{1}{2}i\Gamma(p-2) & 0 & 0 & g_2\sqrt{n-1} & 0 & 0 & 0 \\ g_2\sqrt{n-1} & 0 & 0 & (\delta+\overline{\delta})-\frac{1}{2}i\Gamma(p-3) & -g_2\sqrt{m-1} & 0 & g_1\sqrt{n} & 0 & 0 \\ 0 & g_2\sqrt{n-1} & 0 & -g_2\sqrt{m-1} & -\frac{1}{2}i\Gamma(p-2) & -g_1\sqrt{m} & 0 & g_1\sqrt{n} & 0 \\ 0 & 0 & g_2\sqrt{n-1} & 0 & -g_1\sqrt{m} & (-\delta+\overline{\delta})-\frac{1}{2}i\Gamma(p-1) & 0 & 0 & g_1\sqrt{n} \\ 0 & 0 & 0 & g_1\sqrt{n} & 0 & 0 & +2\delta-\frac{1}{2}i\Gamma(p-2) & -g_2\sqrt{m-1} & 0 \\ 0 & 0 & 0 & 0 & g_1\sqrt{n} & 0 & -g_2\sqrt{m-1} & -(-\delta+\overline{\delta})-\frac{1}{2}i\Gamma(p-1) & -g_1\sqrt{m} \\ 0 & 0 & 0 & 0 & 0 & g_1\sqrt{n} & 0 & -g_1\sqrt{m} & -\frac{1}{2}i\Gamma p \end{bmatrix} \tag{A2}$$

with $p = n + m$, and

$$B(n,m) = -i\Gamma \begin{bmatrix} \sqrt{n-1}\sqrt{m-1} & 0 & 0 & 0 & 0 & 0 & 0 & 0 & 0 \\ 0 & \sqrt{n-1}\sqrt{m} & 0 & 0 & 0 & 0 & 0 & 0 & 0 \\ 0 & 0 & \sqrt{n-1}\sqrt{m+1} & 0 & 0 & 0 & 0 & 0 & 0 \\ 0 & 0 & 0 & \sqrt{n}\sqrt{m-1} & 0 & 0 & 0 & 0 & 0 \\ 0 & 0 & 0 & 0 & \sqrt{n}\sqrt{m} & 0 & 0 & 0 & 0 \\ 0 & 0 & 0 & 0 & 0 & \sqrt{n}\sqrt{m+1} & 0 & 0 & 0 \\ 0 & 0 & 0 & 0 & 0 & 0 & \sqrt{n+1}\sqrt{m-1} & 0 & 0 \\ 0 & 0 & 0 & 0 & 0 & 0 & 0 & \sqrt{n+1}\sqrt{m} & 0 \\ 0 & 0 & 0 & 0 & 0 & 0 & 0 & 0 & \sqrt{n+1}\sqrt{m+1} \end{bmatrix}. \tag{A3}$$

For the $(0,0)$ set we have

$$\rho(0,0) = \begin{bmatrix} \rho_{00;00} \end{bmatrix} \tag{A4}$$

$$A(0,0) = \omega_c(0) \begin{bmatrix} 1 \end{bmatrix} \tag{A5}$$

$$B(0,0) = \begin{bmatrix} 0 & 0 & 0 & -i\Gamma \end{bmatrix}. \tag{A6}$$

For the $(1,0)$ set we have

$$\rho(1,0) = \begin{bmatrix} \rho_{01;00} \\ \rho_{10;00} \end{bmatrix} \tag{A7}$$

$$A(1,0) = \omega_c(1) \begin{bmatrix} 1 & 0 \\ 0 & 1 \end{bmatrix} + \begin{bmatrix} -\delta + \overline{\delta} & g_1 \\ g_1 & -\tfrac{1}{2}i\Gamma \end{bmatrix} \tag{A8}$$

$$B(1,0) = \begin{bmatrix} 0 & 0 & 0 & -i\Gamma & 0 & 0 \\ 0 & 0 & 0 & 0 & 0 & -i\sqrt{2}\Gamma \end{bmatrix}. \tag{A9}$$

For the $(1,1)$ set we have

$$\rho(1,1) = \begin{bmatrix} \rho_{01;01} \\ \rho_{01;10} \\ \rho_{10;01} \\ \rho_{10;10} \end{bmatrix} \tag{A10}$$

$$A(1,1) = \omega_c(0) \begin{bmatrix} 1 & 0 & 0 & 0 \\ 0 & 1 & 0 & 0 \\ 0 & 0 & 1 & 0 \\ 0 & 0 & 0 & 1 \end{bmatrix}$$
$$+ \begin{bmatrix} 0 & -g_1 & g_1 & 0 \\ -g_1 & -\delta + \overline{\delta} - \tfrac{1}{2}i\Gamma & 0 & g_1 \\ g_1 & 0 & +\delta - \overline{\delta} - \tfrac{1}{2}i\Gamma & -g_1 \\ 0 & g_1 & -g_1 & -i\Gamma \end{bmatrix} \tag{A11}$$

$$B(1,1) = \begin{bmatrix} 0 & 0 & 0 & 0 & -i\Gamma & 0 & 0 & 0 & 0 \\ 0 & 0 & 0 & 0 & 0 & -i\sqrt{2}\Gamma & 0 & 0 & 0 \\ 0 & 0 & 0 & 0 & 0 & 0 & 0 & -i\sqrt{2}\Gamma & 0 \\ 0 & 0 & 0 & 0 & 0 & 0 & 0 & 0 & -i2\,\Gamma \end{bmatrix}. \tag{A12}$$

For the $(2,1)$ set we have

$$\rho(2,1) = \begin{bmatrix} \rho_{02;01} \\ \rho_{02;10} \\ \rho_{11;01} \\ \rho_{11;10} \\ \rho_{20;01} \\ \rho_{20;10} \end{bmatrix} \tag{A13}$$

$$A(2,1) = \omega_c(1) \begin{bmatrix} 1 & 0 & 0 & 0 & 0 & 0 \\ 0 & 1 & 0 & 0 & 0 & 0 \\ 0 & 0 & 1 & 0 & 0 & 0 \\ 0 & 0 & 0 & 1 & 0 & 0 \\ 0 & 0 & 0 & 0 & 1 & 0 \\ 0 & 0 & 0 & 0 & 0 & 1 \end{bmatrix}$$
$$+ \begin{bmatrix} -\delta + \overline{\delta} & -g_1 & g_2 & 0 & 0 & 0 \\ -g_1 & -2\delta - \tfrac{1}{2}i\Gamma & 0 & g_2 & 0 & 0 \\ g_2 & 0 & -\tfrac{1}{2}i\Gamma & -g_1 & \sqrt{2}g_1 & 0 \\ 0 & g_2 & -g_1 & -\delta + \overline{\delta} - i\Gamma & 0 & \sqrt{2}g_1 \\ 0 & 0 & \sqrt{2}g_1 & 0 & +\delta - \overline{\delta} - i\Gamma & -g_1 \\ 0 & 0 & 0 & \sqrt{2}g_1 & -g_1 & -\tfrac{3}{2}i\Gamma \end{bmatrix} \tag{A14}$$

$$B(2,1) = \begin{bmatrix} 0 & -i\Gamma & 0 & 0 & 0 & 0 & 0 & 0 \\ 0 & 0 & -i\sqrt{2}\Gamma & 0 & 0 & 0 & 0 & 0 \\ 0 & 0 & 0 & 0 & -i\sqrt{2}\Gamma & 0 & 0 & 0 \\ 0 & 0 & 0 & 0 & 0 & -i2\,\Gamma & 0 & 0 \\ 0 & 0 & 0 & 0 & 0 & 0 & 0 & -i\sqrt{3}\Gamma & 0 \\ 0 & 0 & 0 & 0 & 0 & 0 & 0 & 0 & -i\sqrt{6}\Gamma \end{bmatrix}. \tag{A15}$$

For the $(2,2)$ set we have

$$\rho(2,2) = \begin{bmatrix} \rho_{02;02} \\ \rho_{02;11} \\ \rho_{02;20} \\ \rho_{11;02} \\ \rho_{11;11} \\ \rho_{11;20} \\ \rho_{20;02} \\ \rho_{20;11} \\ \rho_{20;20} \end{bmatrix} \tag{A16}$$

$$A(2,2) \;=\; \omega_c(0) \begin{bmatrix} 1&0&0&0&0&0&0&0&0\\ 0&1&0&0&0&0&0&0&0\\ 0&0&1&0&0&0&0&0&0\\ 0&0&0&1&0&0&0&0&0\\ 0&0&0&0&1&0&0&0&0\\ 0&0&0&0&0&1&0&0&0\\ 0&0&0&0&0&0&1&0&0\\ 0&0&0&0&0&0&0&1&0\\ 0&0&0&0&0&0&0&0&1 \end{bmatrix}$$

$$+ \begin{bmatrix} 0 & -g_2 & 0 & g_2 & 0 & 0 & 0 & 0 & 0\\ -g_2 & -(\delta+\overline{\delta})-\frac{1}{2}i\Gamma & -g_1\sqrt{2} & 0 & g_2 & 0 & 0 & 0 & 0\\ 0 & -g_1\sqrt{2} & -2\delta-i\Gamma & 0 & 0 & g_2 & 0 & 0 & 0\\ g_2 & 0 & 0 & +(\delta+\overline{\delta})-\frac{1}{2}i\Gamma & -g_2 & 0 & g_1\sqrt{2} & 0 & 0\\ 0 & g_2 & 0 & -g_2 & -i\Gamma & -g_1\sqrt{2} & 0 & g_1\sqrt{2} & 0\\ 0 & 0 & g_2 & 0 & -g_1\sqrt{2} & (-\delta+\overline{\delta})-\frac{3}{2}i\Gamma & 0 & 0 & g_1\sqrt{2}\\ 0 & 0 & 0 & g_1\sqrt{2} & 0 & 0 & +2\delta-i\Gamma & -g_2 & 0\\ 0 & 0 & 0 & 0 & g_1\sqrt{2} & 0 & -g_2 & -(-\delta+\overline{\delta})-\frac{3}{2}i\Gamma & -g_1\sqrt{2}\\ 0 & 0 & 0 & 0 & 0 & g_1\sqrt{2} & 0 & -g_1\sqrt{2} & -i2\,\Gamma \end{bmatrix} \tag{A17}$$

$$B(2,2) \;=\; \begin{bmatrix} -i\Gamma & 0 & 0 & 0 & 0 & 0 & 0 & 0 & 0\\ 0 & -i\Gamma\sqrt{2} & 0 & 0 & 0 & 0 & 0 & 0 & 0\\ 0 & 0 & -i\Gamma\sqrt{3} & 0 & 0 & 0 & 0 & 0 & 0\\ 0 & 0 & 0 & -i\Gamma\sqrt{2} & 0 & 0 & 0 & 0 & 0\\ 0 & 0 & 0 & 0 & -i\Gamma\,2 & 0 & 0 & 0 & 0\\ 0 & 0 & 0 & 0 & 0 & -i\Gamma\sqrt{6} & 0 & 0 & 0\\ 0 & 0 & 0 & 0 & 0 & 0 & -i\Gamma\sqrt{3} & 0 & 0\\ 0 & 0 & 0 & 0 & 0 & 0 & 0 & -i\Gamma\sqrt{6} & 0\\ 0 & 0 & 0 & 0 & 0 & 0 & 0 & 0 & -i\Gamma\,3 \end{bmatrix}. \tag{A18}$$

APPENDIX B: SPECTRUM FOR CASE A

For the cascade case A situation we take

$$\widehat{V}_- \;=\; \mu^*\,\widehat{a}$$
$$= \mu^* \sum_{n\nu} \sqrt{n}\,|n-1;\nu\rangle\langle n;\nu| \tag{B1}$$

$$\widehat{V}_+ \;=\; \mu\,\widehat{a}^\dagger$$
$$= \mu \sum_{m\lambda} \sqrt{m}\,|m;\lambda\rangle\langle m-1;\lambda|. \tag{B2}$$

The two time correlation function is then

$$Tr_{SR}\left(\widehat{\rho}_I\,\widehat{V}_+(t_2)\,\widehat{V}_-(t_1)\right)$$
$$= |\mu|^2 \sum_{m\lambda}\sum_{n\nu} \sqrt{m}\sqrt{n}\,\left\langle \widehat{S}_{m\lambda;\,\overline{m-1}\lambda}(t_2)\widehat{S}_{\overline{n-1}\nu;\,n\nu}(t_1)\right\rangle, \tag{B3}$$

where the transition operators $\widehat{S}_{m\lambda;\,n\nu}(t) \equiv |m;\lambda\rangle\langle n;\nu|$ are Heisenberg operators at time t, and the trace is over both system and reservoir states. The two time correlation functions can be evaluated using the quantum regression theorem [12, 40, 41], the results for which is given in terms of the evolution operator matrix elements $U_{m\lambda;\,n\nu::l\beta;\,k\alpha}(\tau)$ associated with the density matrix equations and considered as a function of the time difference $\tau = |t_1 - t_2| \geqslant 0$, and density matrix elements $\rho_{m\lambda;\,n\nu}(t_{1,2})$ considered as a function of the smaller of the two times t_1 and t_2.

We find using the result (31) for $t_2 = t_1 + \tau \geqslant t_1$

$$Tr_{SR}\left(\widehat{\rho}_I\,\widehat{V}_+(t_2)\,\widehat{V}_-(t_1)\right) = |\mu|^2 \sum_{m\lambda}\sum_{n\nu} \sqrt{m}\sqrt{n} \sum_{k\alpha} U_{\overline{m-1}\lambda;\,m\lambda::\overline{n-1}\nu;\,k\alpha}(\tau)\,\rho_{n\nu;\,k\alpha}(t_1), \tag{B4}$$

and using (32) for $t_1 = t_2 + \tau \geqslant t_2$

$$Tr_{SR}\left(\widehat{\rho}_i\,\widehat{V}_+(t_2)\,\widehat{V}_-(t_1)\right) \;=\; |\mu|^2 \sum_{m\lambda}\sum_{n\nu} \sqrt{m}\sqrt{n} \sum_{k\alpha} U_{n\nu;\,\overline{n-1}\nu::k\alpha;\,\overline{m-1}\lambda}(\tau)\,\rho_{k\alpha;\,m\lambda}(t_2)$$
$$= |\mu|^2 \sum_{m\lambda}\sum_{n\nu} \sqrt{m}\sqrt{n} \sum_{k\alpha} U_{m\lambda;\,\overline{m-1}\lambda::k\alpha;\,\overline{n-1}\nu}(\tau)\,\rho_{k\alpha;\,n\nu}(t_2), \tag{B5}$$

where to obtain the last result we have made the interchange $m\lambda \leftrightarrow n\nu$.

Substituting into the result for the spectrum we have

$$
\begin{aligned}
S(\omega) &= \frac{1}{\hbar^2}\left[\iint_0^\infty dt_1 dt_2 \exp i\omega(t_1-t_2) Tr_S\left(\widehat{\rho}_i\,\widehat{V}_+(t_2)\,\widehat{V}_-(t_1)\right)\right]_{t_1\geqslant t_2} \\
&\quad + \frac{1}{\hbar^2}\left[\iint_0^\infty dt_1 dt_2 \exp i\omega(t_1-t_2) Tr_S\left(\widehat{\rho}_i\,\widehat{V}_+(t_2)\,\widehat{V}_-(t_1)\right)\right]_{t_2\geqslant t_1} \\
S(\omega) &= \frac{|\mu|^2}{\hbar^2}\sum_{m\lambda}\sum_{n\nu}\sqrt{m}\sqrt{n}\sum_{k\alpha}\int_0^\infty dt_2\int_{t_2}^\infty dt_1 \exp i\omega(t_1-t_2)\,U_{m\lambda;\,\overline{m-1}\lambda::k\alpha;\,\overline{n-1}\nu}(\tau)\,\rho_{k\alpha;\,n\nu}(t_2) \\
&\quad + \frac{|\mu|^2}{\hbar^2}\sum_{m\lambda}\sum_{n\nu}\sqrt{m}\sqrt{n}\sum_{k\alpha}\int_0^\infty dt_1\int_{t_1}^\infty dt_2 \exp i\omega(t_1-t_2)\,U_{\overline{m-1}\lambda;\,m\lambda::\overline{n-1}\nu;\,k\alpha}(\tau)\,\rho_{n\nu;\,k\alpha}(t_1) \\
S(\omega) &= \frac{|\mu|^2}{\hbar^2}\sum_{m\lambda}\sum_{n\nu}\sqrt{m}\sqrt{n}\sum_{k\alpha}\int_0^\infty dt_2\int_0^\infty d\tau\,\exp(i\omega\tau)\,U_{m\lambda;\,\overline{m-1}\lambda::k\alpha;\,\overline{n-1}\nu}(\tau)\,\rho_{k\alpha;\,n\nu}(t_2) \\
&\quad + \frac{|\mu|^2}{\hbar^2}\sum_{m\lambda}\sum_{n\nu}\sqrt{m}\sqrt{n}\sum_{k\alpha}\int_0^\infty dt_1\int_0^\infty d\tau\,\exp(-i\omega\tau)\,U_{\overline{m-1}\lambda;\,m\lambda::\overline{n-1}\nu;\,k\alpha}(\tau)\,\rho_{n\nu;\,k\alpha}(t_1).
\end{aligned}
$$

(B6)

To obtain the last expression, the integration variables have been changed in the first region ($t_1 \geqslant t_2$) to τ, t_2 via the transformation $t_1 = \tau + t_2, t_2 = t_2$ (so the Jacobian equals $+1$) and in the second region ($t_2 \geqslant t_1$) to t_1, τ via the transformation $t_1 = t_1, t_2 = \tau + t_1$ (so the Jacobian equals $+1$).

Since by taking the complex conjugate of the density matrix equations we have

$$
\rho_{k\alpha;\,n\nu}(t) = \rho_{n\nu;\,k\alpha}(t)^* \tag{B7}
$$
$$
U_{m\lambda;\,\overline{m-1}\lambda::k\alpha;\,\overline{n-1}\nu}(\tau) = U_{\overline{m-1}\lambda;\,m\lambda::\overline{n-1}\nu;\,k\alpha}(\tau)^*, \tag{B8}
$$

it is not difficult to see that the second term in the last equation is just the complex conjugate of the first, thus proving that our result for the spectrum is real.

For each contribution the double integrals factorise, each giving a Laplace transform—albeit for s on the imaginary axis (which may need to be written as a limiting process). We find that

$$
\begin{aligned}
S(\omega) &= \frac{|\mu|^2}{\hbar^2}\sum_{m\lambda}\sum_{n\nu}\sqrt{m}\sqrt{n}\sum_{k\alpha}\widetilde{U}_{m\lambda;\,\overline{m-1}\lambda::k\alpha;\,\overline{n-1}\nu}(-i\omega+\epsilon)\,\widetilde{\rho}_{k\alpha;\,n\nu}(\epsilon') \\
&\quad + \frac{|\mu|^2}{\hbar^2}\sum_{m\lambda}\sum_{n\nu}\sqrt{m}\sqrt{n}\sum_{k\alpha}\widetilde{U}_{\overline{m-1}\lambda;\,m\lambda::\overline{n-1}\nu;\,k\alpha}(+i\omega+\epsilon)\,\widetilde{\rho}_{n\nu;\,k\alpha}(\epsilon') \\
&= 2\,\mathrm{Re}\,\frac{|\mu|^2}{\hbar^2}\sum_{m\lambda}\sum_{n\nu}\sqrt{m}\sqrt{n}\sum_{k\alpha}\widetilde{U}_{m\lambda;\,\overline{m-1}\lambda::k\alpha;\,\overline{n-1}\nu}(-i\omega+\epsilon)\,\widetilde{\rho}_{k\alpha;\,n\nu}(\epsilon'),
\end{aligned}
$$

(B9)

where the limits $\epsilon, \epsilon' \to 0$ are understood. The last result follows from the second term being the complex conjugate of the first.

The initial conditions will lead to restrictions on the terms to be summed over. Of course the quantities α, λ, ν already only sum over the three atomic states. As shown previously for the present initial conditions, the only non zero $\rho_{k\alpha;\,n\nu}(t)$ are those in the $(2,2)$, $(1,1)$ and $(0,0)$

coupled sets—for $(2,2)$ these are $\rho_{02;\,02}$, $\rho_{02;\,11}$, $\rho_{02;\,20}$, $\rho_{11;\,02}$, $\rho_{11;\,11}$, $\rho_{11;\,20}$, $\rho_{20;\,02}$, $\rho_{20;\,11}$ and $\rho_{20;\,20}$; for the $(1,1)$ set we have $\rho_{01;\,01}, \rho_{01;\,10}, \rho_{10;\,01}$ and $\rho_{10;\,10}$ and for the $(0,0)$ set we have $\rho_{00;\,00}(t)$—corresponding to the system states $|0;2\rangle$, $|1;1\rangle$ and $|0;1\rangle$ being the only ones populated during the decay process. This will restrict the sums over k, n, and the $\widetilde{\rho}_{k\alpha;\,n\nu}(\epsilon')$ that are involved are all Laplace transforms of members of the $(2,2)$, $(1,1)$ and

$(0,0)$ sets for the $\rho(n,m,t)$. In fact given that we also require $n \geqslant 1$ due to the $\sqrt{n}$, factor, the only $\widetilde{\rho}_{k\alpha;\,n\nu}(\epsilon')$ that are possible are $\widetilde{\rho}_{02;\,11}$, $\widetilde{\rho}_{02;\,20}$, $\widetilde{\rho}_{11;\,11}$, $\widetilde{\rho}_{11;\,20}$, $\widetilde{\rho}_{20;\,11}$, $\widetilde{\rho}_{20;\,20}$, which are all in the $(2,2)$ coupled set and $\widetilde{\rho}_{01;\,10}$, $\widetilde{\rho}_{10;\,10}$ which are in the $(1,1)$ coupled set. This then restricts the $\widetilde{U}_{m\lambda;\,\overline{m-1}\lambda::k\alpha;\,\overline{n-1}\nu}(-i\omega + \epsilon)$ to be of the form $\widetilde{U}_{m\lambda;\,\overline{m-1}\lambda::02;\,01}(-i\omega + \epsilon)$, $\widetilde{U}_{m\lambda;\,\overline{m-1}\lambda::02;\,10}(-i\omega + \epsilon)$, $\widetilde{U}_{m\lambda;\,\overline{m-1}\lambda::11;\,01}(-i\omega + \epsilon)$, $\widetilde{U}_{m\lambda;\,\overline{m-1}\lambda::11;\,10}(-i\omega + \epsilon)$, $\widetilde{U}_{m\lambda;\,\overline{m-1}\lambda::20;\,01}(-i\omega + \epsilon)$, $\widetilde{U}_{m\lambda;\,\overline{m-1}\lambda::20;\,10}(-i\omega + \epsilon)$ and $\widetilde{U}_{m\lambda;\,\overline{m-1}\lambda::01;\,00}(-i\omega + \epsilon)$, $\widetilde{U}_{m\lambda;\,\overline{m-1}\lambda::10;\,00}(-i\omega + \epsilon)$ be-

cause of the k,n restriction (note the $\overline{n-1}\nu$ in the subscript). Since $\rho_{02;\,01}$, $\rho_{02;\,10}$, $\rho_{11;\,01}$, $\rho_{11;\,10}$, $\rho_{20;\,01}$, $\rho_{20;\,10}$ are all in the $(2,1)$ set these are Laplace transforms of the $U_{n,m::2,1}(t)$. The other terms $\rho_{01;\,00}$, $\rho_{10;\,00}$ are both in the $(1,0)$ set these are Laplace transforms of the $U_{n,m::1,0}(t)$. The spectrum can be broken up into two contributions, $S_6(\omega)$ which is associated with $\widetilde{\rho}_{k\alpha;\,n\nu}(\epsilon')$ for the $(2,2)$ coupled set and $S_2(\omega)$ which is associated with $\widetilde{\rho}_{k\alpha;\,n\nu}(\epsilon')$ for the $(1,1)$ coupled set. This gives

$$
\begin{aligned}
S(\omega) &= 2\,\mathrm{Re}\,\frac{|\mu|^2}{\hbar^2}\sum_{m\geqslant 1,\lambda}\sum_{n\geqslant 1,\nu}\sqrt{m}\sqrt{n}\sum_{k\alpha}\widetilde{U}_{m\lambda;\,\overline{m-1}\lambda::k\alpha;\,\overline{n-1}\nu}(-i\omega+\epsilon)\,\widetilde{\rho}_{k\alpha;\,n\nu}(\epsilon')\\
&= S_6(\omega) + S_2(\omega)
\end{aligned}
\tag{B10}
$$

$$
\begin{aligned}
S_6(\omega) &= 2\,\mathrm{Re}\,\frac{|\mu|^2}{\hbar^2}\sum_{m\geqslant 1,\lambda}\sqrt{m}\sqrt{1}\widetilde{U}_{m\lambda;\,\overline{m-1}\lambda::02;\,01}(-i\omega+\epsilon)\,\widetilde{\rho}_{02;\,11}(\epsilon')\\
&\quad + 2\,\mathrm{Re}\,\frac{|\mu|^2}{\hbar^2}\sum_{m\geqslant 1,\lambda}\sqrt{m}\sqrt{2}\widetilde{U}_{m\lambda;\,\overline{m-1}\lambda::02;\,10}(-i\omega+\epsilon)\,\widetilde{\rho}_{02;\,20}(\epsilon')\\
&\quad + 2\,\mathrm{Re}\,\frac{|\mu|^2}{\hbar^2}\sum_{m\geqslant 1,\lambda}\sqrt{m}\sqrt{1}\widetilde{U}_{m\lambda;\,\overline{m-1}\lambda::11;\,01}(-i\omega+\epsilon)\,\widetilde{\rho}_{11;\,11}(\epsilon')\\
&\quad + 2\,\mathrm{Re}\,\frac{|\mu|^2}{\hbar^2}\sum_{m\geqslant 1,\lambda}\sqrt{m}\sqrt{2}\widetilde{U}_{m\lambda;\,\overline{m-1}\lambda::11;\,10}(-i\omega+\epsilon)\,\widetilde{\rho}_{11;\,20}(\epsilon')\\
&\quad + 2\,\mathrm{Re}\,\frac{|\mu|^2}{\hbar^2}\sum_{m\geqslant 1,\lambda}\sqrt{m}\sqrt{1}\widetilde{U}_{m\lambda;\,\overline{m-1}\lambda::20;\,01}(-i\omega+\epsilon)\,\widetilde{\rho}_{20;\,11}(\epsilon')\\
&\quad + 2\,\mathrm{Re}\,\frac{|\mu|^2}{\hbar^2}\sum_{m\geqslant 1,\lambda}\sqrt{m}\sqrt{2}\widetilde{U}_{m\lambda;\,\overline{m-1}\lambda::20;\,10}(-i\omega+\epsilon)\,\widetilde{\rho}_{20;\,20}(\epsilon')\\
S_2(\omega) &= 2\,\mathrm{Re}\,\frac{|\mu|^2}{\hbar^2}\sum_{m\geqslant 1,\lambda}\sqrt{m}\sqrt{1}\,\widetilde{U}_{m\lambda;\,\overline{m-1}\lambda::01;\,00}(-i\omega+\epsilon)\,\widetilde{\rho}_{01;\,10}(\epsilon')\\
&\quad + 2\,\mathrm{Re}\,\frac{|\mu|^2}{\hbar^2}\sum_{m\geqslant 1,\lambda}\sqrt{m}\sqrt{1}\,\widetilde{U}_{m\lambda;\,\overline{m-1}\lambda::10;\,00}(-i\omega+\epsilon)\,\widetilde{\rho}_{10;\,10}(\epsilon').
\end{aligned}
\tag{B11}
$$

The six $S_6(\omega)$ terms involve $\widetilde{U}_{n,m::2,1}(-i\omega + \epsilon)$ and the two $S_2(\omega)$ terms involve $\widetilde{U}_{n,m::1,0}(-i\omega + \epsilon)$. Then because the possible $U_{n,m::2,1}(t)$ and $U_{n,m::1,0}(t)$ must be such that $n = m + 1$, we see that the non-zero $\widetilde{U}_{m\lambda;\,\overline{m-1}\lambda::k\alpha;\,\overline{n-1}\nu}(-i\omega + \epsilon)$ for the first six $S_6(\omega)$ terms $\widetilde{U}_{n,m::2,1}(-i\omega + \epsilon)$ must all be Laplace transforms from the sets of matrices $U_{1,0::2,1}(t), U_{2,1::2,1}(t), U_{3,2::2,1}(t), U_{4,3::2,1}(t), \ldots$ and the the non-zero $\widetilde{U}_{m\lambda;\,\overline{m-1}\lambda::k\alpha;\,\overline{n-1}\nu}(-i\omega + \epsilon)$ for the last two $S_2(\omega)$ terms $\widetilde{U}_{n,m::1,0}(-i\omega + \epsilon)$ must all be Laplace transforms from the sets of matrices $U_{1,0::1,0}(t), U_{2,1::1,0}(t), U_{3,2::1,0}(t), U_{4,3::1,0}(t), \ldots$

However, for the first six $S_6(\omega)$ terms we see from the Laplace transforms

$$
\begin{aligned}
(s + iA(1,0))\,\widetilde{U}(1, 0 :: 2, 1) - iB(1,0)\,\widetilde{U}(2, 1 :: 2, 1) &= 0\\
(s + iA(2,1))\,\widetilde{U}(2, 1 :: 2, 1) - iB(2,1)\,\widetilde{U}(3, 2 :: 2, 1) &= E_6\\
(s + iA(3,2))\,\widetilde{U}(3, 2 :: 2, 1) - iB(3,2)\,\widetilde{U}(4, 3 :: 2, 1) &= 0\\
(s + iA(4,3))\,\widetilde{U}(4, 3 :: 2, 1) - iB(4,3)\,\widetilde{U}(5, 4 :: 2, 1) &= 0
\end{aligned}
\tag{B12}
$$

and it is easy to see that the solution to these equations is

$$\widetilde{U}(2,1::2,1;s) = (s+iA(2,1))^{-1}$$
$$\widetilde{U}(1,0::2,1;s) = (s+iA(1,0))^{-1}$$
$$\times iB(1,0)\,(s+iA(2,1))^{-1}$$
$$\widetilde{U}(n+1,n::2,1;s) = 0 \qquad (n>1). \qquad \text{(B13)}$$

This solution corresponds to the previous result that an initial density matrix with only non-zero elements in the (N,M) set or below cannot evolve into a density matrix with non-zero elements in sets such as $(N+1,M+1)$, $(N+2,M+2),\dots$, due to the irreversible nature of the relaxation processes. This means that for the first six $S_6(\omega)$ terms the $\widetilde{U}_{m\lambda;\overline{m-1}\lambda::k\alpha;\overline{n-1}\nu}(-i\omega+\epsilon)$ must be from the $U_{2,1::2,1}(t)$ and $U_{1,0::2,1}(t)$ matrix elements only, and this places a restriction on m and λ. Since the only density matrix element in the $(1,0)$ set of the form $\rho_{m\lambda;\overline{m-1}\lambda}$ is $\rho_{10;00}$ then in fact the only terms are for $m=1$ and $\lambda=0$ (namely $\widetilde{U}_{10,00::02;01}(-i\omega+\epsilon)$, $\widetilde{U}_{10,00::02;10}(-i\omega+\epsilon)$, $\widetilde{U}_{10,00::11;01}(-i\omega+\epsilon)$, $\widetilde{U}_{10,00::11;10}(-i\omega+\epsilon)$, $\widetilde{U}_{10,00::20;01}(-i\omega+\epsilon)$ and $\widetilde{U}_{10,00::20,10}(-i\omega+\epsilon)$). Since the only density matrix elements in the $(2,1)$ set of the form $\rho_{m\lambda;\overline{m-1}\lambda}$ are $\rho_{11;01}$ and $\rho_{20;10}$ then the only terms are for $m=1$ and $\lambda=1$ or $m=2$ and $\lambda=0$, (namely $\widetilde{U}_{11,01::02;01}(-i\omega+\epsilon)$, $\widetilde{U}_{11,01::02;10}(-i\omega+\epsilon)$, $\widetilde{U}_{11,01::11;01}(-i\omega+\epsilon)$, $\widetilde{U}_{11,01::11;10}(-i\omega+\epsilon)$, $\widetilde{U}_{11,01::20;01}(-i\omega+\epsilon)$ and $\widetilde{U}_{11,01::20,10}(-i\omega+\epsilon)$ for $m=1$ and $\lambda=1$; then $\widetilde{U}_{20,10::02;01}(-i\omega+\epsilon)$, $\widetilde{U}_{20,10::02;10}(-i\omega+\epsilon)$, $\widetilde{U}_{20,10::11;01}(-i\omega+\epsilon)$,

$\widetilde{U}_{20,10::11;10}(-i\omega+\epsilon)$, $\widetilde{U}_{20,10::20;01}(-i\omega+\epsilon)$ and $\widetilde{U}_{20,10::20,10}(-i\omega+\epsilon)$ for $m=2$ and $\lambda=0$). Thus each of the first six $S_6(\omega)$ terms produces three contributions.

Also, for the last two $S_2(\omega)$ terms we see from the Laplace transform equations

$$(s+iA(1,0))\,\widetilde{U}(1,0\;:\;:1,0) - iB(1,0)\,\widetilde{U}(2,1::1,0) = E_2$$
$$(s+iA(2,1))\,\widetilde{U}(2,1\;:\;:1,0) - iB(2,1)\,\widetilde{U}(3,2::1,0) = 0$$
$$(s+iA(3,2))\,\widetilde{U}(3,2\;:\;:1,0) - iB(3,2)\,\widetilde{U}(4,3::1,0) = 0$$
$$\cdots \qquad \text{(B14)}$$

and it is easy to see that the solution to these equations is

$$\widetilde{U}(1,0\;:\;:1,0;s) = (s+iA(1,0))^{-1}$$
$$\widetilde{U}(n+1,n\;:\;:1,0;s) = 0 \qquad (n>1), \qquad \text{(B15)}$$

from the same considerations as for the first six $S_6(\omega)$ terms. This means that for the last two $S_2(\omega)$ terms the $\widetilde{U}_{m\lambda;\overline{m-1}\lambda::k\alpha;\overline{n-1}\nu}(-i\omega+\epsilon)$ must be from the $U_{1,0::1,0}(t)$ only, and this places a restriction on m and λ. Since the only density matrix element in the $(1,0)$ set of the form $\rho_{m\lambda;\overline{m-1}\lambda}$ is $\rho_{10;00}$ then in fact the only terms are for $m=1$ and $\lambda=0$ (namely $\widetilde{U}_{10;00::01,00}(-i\omega+\epsilon)$ and $\widetilde{U}_{10;00::10,00}(-i\omega+\epsilon)$). Each of the two $S_2(\omega)$ terms produces one contribution only.

We finally have for the spectrum

$$S(\omega) = S_2(\omega) + S_6(\omega) \qquad \text{(B16)}$$

$$S_2(\omega) = 2\,\mathrm{Re}\,\frac{|\mu|^2}{\hbar^2}\sqrt{1}\sqrt{1}\{\widetilde{\rho}_{10;10}(\epsilon')\widetilde{U}_{10;00::01;00}(-i\omega+\epsilon) + \widetilde{\rho}_{01;10}(\epsilon')\widetilde{U}_{10;00::10;00}(-i\omega+\epsilon)\}$$

$$\begin{aligned}
S_6(\omega) = {}& 2\,\mathrm{Re}\,\frac{|\mu|^2}{\hbar^2} \\
& \times [\sqrt{1}\,\widetilde{\rho}_{02;11}(\epsilon')\{\sqrt{1}\widetilde{U}_{10,00::02;01}(-i\omega+\epsilon) + \sqrt{1}\widetilde{U}_{11,01::02;01}(-i\omega+\epsilon) \\
& + \sqrt{2}\widetilde{U}_{20,10::02;01}(-i\omega+\epsilon)\} \\
& + \sqrt{2}\,\widetilde{\rho}_{02;20}(\epsilon')\{\sqrt{1}\widetilde{U}_{10,00::02;10}(-i\omega+\epsilon) + \sqrt{1}\widetilde{U}_{11,01::02;10}(-i\omega+\epsilon) \\
& + \sqrt{2}\widetilde{U}_{20,10::02;10}(-i\omega+\epsilon)\} \\
& + \sqrt{1}\,\widetilde{\rho}_{11;11}(\epsilon')\{\sqrt{1}\widetilde{U}_{10,00::11;01}(-i\omega+\epsilon) + \sqrt{1}\widetilde{U}_{11,01::11;01}(-i\omega+\epsilon) \\
& + \sqrt{2}\widetilde{U}_{20,10::11,01}(-i\omega+\epsilon)\} \\
& + \sqrt{2}\,\widetilde{\rho}_{11;20}(\epsilon')\{\sqrt{1}\widetilde{U}_{10,00::11,10}(-i\omega+\epsilon) + \sqrt{1}\widetilde{U}_{11,01::11,10}(-i\omega+\epsilon) \\
& + \sqrt{2}\widetilde{U}_{20,10::11;10}(-i\omega+\epsilon)\} \\
& + \sqrt{1}\,\widetilde{\rho}_{20;11}(\epsilon')\{\sqrt{1}\widetilde{U}_{10,00::20;01}(-i\omega+\epsilon) + \sqrt{1}\widetilde{U}_{11,01::20;01}(-i\omega+\epsilon) \\
& + \sqrt{2}\widetilde{U}_{20,10::20;01}(-i\omega+\epsilon)\} \\
& + \sqrt{2}\,\widetilde{\rho}_{20;20}(\epsilon')\{\sqrt{1}\widetilde{U}_{10,00::20,10}(-i\omega+\epsilon) + \sqrt{1}\widetilde{U}_{11,01::20,10}(-i\omega+\epsilon) \\
& + \sqrt{2}\widetilde{U}_{20,10::20,10}(-i\omega+\epsilon)\}].
\end{aligned}$$
$$\text{(B17)}$$

APPENDIX C: SPECTRUM FOR CASE B

For the cascade case B we have

$$\widehat{V}_- = \int d\Delta\, \rho_C(\Delta)\, \mu^*(\Delta)\widehat{b}(\Delta), \qquad (C1)$$

where $\mu^*(\Delta)$ is also a slowly varying function of Δ.

The Heisenberg equations of motion for the Heisenberg operators $\widehat{b}(\Delta, t)$ and $\widehat{a}(t)$ are

$$\frac{d}{dt}\widehat{b}(\Delta, t) = -i\Delta\widehat{b}(\Delta, t) - iW^*(\Delta)\widehat{a}(t) \qquad (C2)$$

$$\frac{d}{dt}\widehat{a}(t) = -i\omega_c\widehat{a}(t) - i\frac{1}{2}g\,\widehat{\sigma}_-(t)$$
$$-i\int d\Delta\, \rho_C(\Delta)\, W(\Delta)\widehat{b}(\Delta, t), \quad (C3)$$

and we easily obtain the formal solution of the first equation as

$$\widehat{b}(\Delta, t) = \exp(-i\Delta t)\widehat{b}(\Delta, 0)$$
$$-iW^*(\Delta)\int_0^t d\tau\, \exp(-i\Delta\tau)\,\widehat{a}(t-\tau). \qquad (C4)$$

If there were no coupling terms, the free evolution for $\widehat{a}(t)$ follows from the second equation to be $\widehat{a}(t) = \widehat{a}(0)\exp(-i\omega_c t)$.

Hence we see that $\widehat{V}_-$ is the sum of a free field term $\widehat{V}_-^F$ and a cavity term $\widehat{V}_-^C$, where

$$\widehat{V}_- = \widehat{V}_-^F + \widehat{V}_-^C \qquad (C5)$$

$$\widehat{V}_-^F = \int d\Delta\, \rho_C(\Delta)\, \mu^*(\Delta)\, \exp(-i\Delta t)\widehat{b}(\Delta) \qquad (C6)$$

$$\widehat{V}_-^C = \int_0^t d\tau\, \left(-i\int d\Delta\, \rho_C(\Delta)\, \mu^*(\Delta)\, W^*(\Delta)\, \exp(-i\Delta\tau)\right)\widehat{a}(t-\tau). \qquad (C7)$$

For the cavity contribution $\widehat{V}_-^C$ the quantity $F(\tau) = \left(-i\int d\Delta\, \rho_C(\Delta)\, \mu^*(\Delta)\, W^*(\Delta)\, \exp(-i\Delta\tau)\right)$ involves slowly varying factors $\rho_C(\Delta)$, $\mu^*(\Delta)$ and $W^*(\Delta)$, so it is not difficult to see that if the frequency width of the product of these factors is Δ_C then the overall quantity $F(\tau)$ decreases to zero over a time scale $\tau_C \sim 1/\Delta_C$. We can then invoke the Markoff approximation on the basis that τ_C is small compared to evolution times for the system and approximate $\widehat{a}(t-\tau)$ over the small timescale τ_C over which the quantity $F(\tau)$ is non-zero by its free evolution expression $\widehat{a}(t-\tau) \doteq \widehat{a}(t)\exp(+i\omega_c\tau)$. Extending the τ integral to ∞ and introducing the usual integrating factor $\exp(-\epsilon\tau)$ gives the following Markovian result for $\widehat{V}_-^C$

$$\widehat{V}_-^C = M^*\widehat{a}, \qquad (C8)$$

where

$$M^* = \int d\Delta\, \frac{\rho_C(\Delta)\, \mu^*(\Delta)\, W^*(\Delta)}{\omega_c - \Delta + i\epsilon} \qquad (C9)$$

is an effective dipole coupling constant. Thus the cavity contribution $\widehat{V}_-^C$ to the spectral quantity $\widehat{V}_-$ is the same as for Case A, apart from a constant of proportionality.

APPENDIX D: SPECTRUM FOR CASE C

For the cascade Case C we have

$$\widehat{V}_- = R_2^*\widehat{\sigma}_2^- + R_1^*\widehat{\sigma}_1^- \qquad (D1)$$
$$= R_2^*\sum_n |n;1\rangle\langle n;2| + R_1^*\sum_n |n;0\rangle\langle n;1| \quad (D2)$$

$$\widehat{V}_+ = R_2\widehat{\sigma}_2^+ + R_1\widehat{\sigma}_1^+ \qquad (D3)$$
$$= R_2\sum_m |m;2\rangle\langle m;1| + R_1\sum_m |m;1\rangle\langle m;0|, \qquad (D4)$$

where henceforth we will choose R_1 and R_2 to be real. Hence the two-time correlation function is

$$Tr_{SR}\left(\widehat{\rho}_I\, \widehat{V}_+(t_2)\, \widehat{V}_-(t_1)\right)$$
$$= R_2^2\sum_m\sum_n \left\langle \widehat{S}_{m2;\,m1}(t_2)\widehat{S}_{n1;\,n2}(t_1)\right\rangle$$
$$+R_1^2\sum_m\sum_n \left\langle \widehat{S}_{m1;\,m0}(t_2)\widehat{S}_{n0;\,n1}(t_1)\right\rangle$$
$$+R_2R_1\sum_m\sum_n \left\langle \widehat{S}_{m2;\,m1}(t_2)\widehat{S}_{n0;\,n1}(t_1)\right\rangle$$
$$+R_1R_2\sum_m\sum_n \left\langle \widehat{S}_{m1;\,m0}(t_2)\widehat{S}_{n1;\,n2}(t_1)\right\rangle. \qquad (D5)$$

For the first term using the quantum regression theorem result (31) we find that for $t_2 = t_1 + \tau \geqslant t_1$

$$R_2^2 \sum_m \sum_n \left\langle \widehat{S}_{m2;\,m1}(t_2) \widehat{S}_{n1;\,n2}(t_1) \right\rangle$$
$$= R_2^2 \sum_m \sum_n \sum_{k\alpha} U_{m1;\,m2::n1;\,k\alpha}(\tau)\, \rho_{n2;\,k\alpha}(t_1),$$

(D6)

and using (32) for $t_1 = t_2 + \tau \geqslant t_2$

$$R_2^2 \sum_m \sum_n \left\langle \widehat{S}_{m2;\,m1}(t_2) \widehat{S}_{n1;\,n2}(t_1) \right\rangle$$
$$= R_2^2 \sum_m \sum_n \sum_{k\alpha} U_{n2;\,n1::k\alpha;\,m1}(\tau)\, \rho_{k\alpha;\,m2}(t_2)$$
$$= R_2^2 \sum_m \sum_n \sum_{k\alpha} U_{m2;\,m1::k\alpha;\,n1}(\tau)\, \rho_{k\alpha;\,n2}(t_2).$$

(D7)

For the second term using the quantum regression theorem we find that for $t_2 = t_1 + \tau \geqslant t_1$

$$R_1^2 \sum_m \sum_n \left\langle \widehat{S}_{m1;\,m0}(t_2) \widehat{S}_{n0;\,n1}(t_1) \right\rangle$$
$$= R_1^2 \sum_m \sum_n \sum_{k\alpha} U_{m0;\,m1::n0;\,k\alpha}(\tau)\, \rho_{n1;\,k\alpha}(t_1),$$

(D8)

and for $t_1 = t_2 + \tau \geqslant t_2$

$$R_1^2 \sum_m \sum_n \left\langle \widehat{S}_{m1;\,m0}(t_2) \widehat{S}_{n0;\,n1}(t_1) \right\rangle$$
$$= R_1^2 \sum_m \sum_n \sum_{k\alpha} U_{n1;\,n0::k\alpha;\,m0}(\tau)\, \rho_{k\alpha;\,m1}(t_2)$$
$$= R_1^2 \sum_m \sum_n \sum_{k\alpha} U_{m1;\,m0::k\alpha;\,n0}(\tau)\, \rho_{k\alpha;\,n1}(t_2).$$

(D9)

For the third term using the quantum regression theorem we find that for $t_2 = t_1 + \tau \geqslant t_1$

$$R_2 R_1 \sum_m \sum_n \left\langle \widehat{S}_{m2;\,m1}(t_2) \widehat{S}_{n0;\,n1}(t_1) \right\rangle$$
$$= R_2 R_1 \sum_m \sum_n \sum_{k\alpha} U_{m1;\,m2::n0;\,k\alpha}(\tau)\, \rho_{n1;\,k\alpha}(t_1),$$

(D10)

and for $t_1 = t_2 + \tau \geqslant t_2$

$$R_2 R_1 \sum_m \sum_n \left\langle \widehat{S}_{m2;\,m1}(t_2) \widehat{S}_{n0;\,n1}(t_1) \right\rangle$$
$$= R_2 R_1 \sum_m \sum_n \sum_{k\alpha} U_{n1;\,n0::k\alpha;\,m1}(\tau)\, \rho_{k\alpha;\,m2}(t_2)$$
$$= R_2 R_1 \sum_m \sum_n \sum_{k\alpha} U_{m1;\,m0::k\alpha;\,n1}(\tau)\, \rho_{k\alpha;\,n2}(t_2).$$

(D11)

For the fourth term using the quantum regression theorem we find that for $t_2 = t_1 + \tau \geqslant t_1$

$$R_1 R_2 \sum_m \sum_n \left\langle \widehat{S}_{m1;\,m0}(t_2) \widehat{S}_{n1;\,n2}(t_1) \right\rangle$$
$$= R_1 R_2 \sum_m \sum_n \sum_{k\alpha} U_{m0;\,m1::n1;\,k\alpha}(\tau)\, \rho_{n2;\,k\alpha}(t_1),$$

(D12)

and for $t_1 = t_2 + \tau \geqslant t_2$

$$R_1 R_2 \sum_m \sum_n \left\langle \widehat{S}_{m1;\,m0}(t_2) \widehat{S}_{n1;\,n2}(t_1) \right\rangle$$
$$= R_1 R_2 \sum_m \sum_n \sum_{k\alpha} U_{n2;\,n1::k\alpha;\,m0}(\tau)\, \rho_{k\alpha;\,m1}(t_2)$$
$$= R_1 R_2 \sum_m \sum_n \sum_{k\alpha} U_{m2;\,m1::k\alpha;\,n0}(\tau)\, \rho_{k\alpha;\,n1}(t_2).$$

(D13)

For the spectrum we have

$$S(\omega) = \frac{1}{\hbar^2} \left[\iint_0^\infty dt_1 dt_2 \exp i\omega(t_1 - t_2) Tr_S \left(\widehat{\rho}_i \, \widehat{V}_+(t_2)\, \widehat{V}_-(t_1) \right) \right]_{t_1 \geqslant t_2}$$
$$+ \frac{1}{\hbar^2} \left[\iint_0^\infty dt_1 dt_2 \exp i\omega(t_1 - t_2) Tr_S \left(\widehat{\rho}_i \, \widehat{V}_+(t_2)\, \widehat{V}_-(t_1) \right) \right]_{t_2 \geqslant t_1},$$

and substituting gives

$$S(\omega) = S(\omega)_{t_1 \geqslant t_2} + S(\omega)_{t_2 \geqslant t_1}$$

$$S(\omega)_{t_1 \geqslant t_2} = \frac{R_2^2}{\hbar^2} \sum_m \sum_n \sum_{k\alpha} \int_0^\infty dt_2 \int_{t_2}^\infty dt_1 \exp i\omega(t_1 - t_2) \, U_{m2;\, m1::k\alpha;\, n1}(\tau)\, \rho_{k\alpha;\, n2}(t_2)$$

$$+ \frac{R_1^2}{\hbar^2} \sum_m \sum_n \sum_{k\alpha} \int_0^\infty dt_2 \int_{t_2}^\infty dt_1 \exp i\omega(t_1 - t_2) \, U_{m1;\, m0::k\alpha;\, n0}(\tau)\, \rho_{k\alpha;\, n1}(t_2)$$

$$+ \frac{R_2 R_1}{\hbar^2} \sum_m \sum_n \sum_{k\alpha} \int_0^\infty dt_2 \int_{t_2}^\infty dt_1 \exp i\omega(t_1 - t_2) \, U_{m1;\, m0::k\alpha;\, n1}(\tau)\, \rho_{k\alpha;\, n2}(t_2)$$

$$+ \frac{R_1 R_2}{\hbar^2} \sum_m \sum_n \sum_{k\alpha} \int_0^\infty dt_2 \int_{t_2}^\infty dt_1 \exp i\omega(t_1 - t_2) \, U_{m2;\, m1::k\alpha;\, n0}(\tau)\, \rho_{k\alpha;\, n1}(t_2)$$

$$S(\omega)_{t_2 \geqslant t_1} = \frac{R_2^2}{\hbar^2} \sum_m \sum_n \sum_{k\alpha} \int_0^\infty dt_1 \int_{t_1}^\infty dt_2 \exp i\omega(t_1 - t_2) \, U_{m1;\, m2::n1;\, k\alpha}(\tau)\, \rho_{n2;\, k\alpha}(t_1)$$

$$+ \frac{R_1^2}{\hbar^2} \sum_m \sum_n \sum_{k\alpha} \int_0^\infty dt_1 \int_{t_1}^\infty dt_2 \exp i\omega(t_1 - t_2) \, U_{m0;\, m1::n0;\, k\alpha}(\tau)\, \rho_{n1;\, k\alpha}(t_1)$$

$$+ \frac{R_2 R_1}{\hbar^2} \sum_m \sum_n \sum_{k\alpha} \int_0^\infty dt_1 \int_{t_1}^\infty dt_2 \exp i\omega(t_1 - t_2) \, U_{m1;\, m2::n0;\, k\alpha}(\tau)\, \rho_{n1;\, k\alpha}(t_1)$$

$$+ \frac{R_1 R_2}{\hbar^2} \sum_m \sum_n \sum_{k\alpha} \int_0^\infty dt_1 \int_{t_1}^\infty dt_2 \exp i\omega(t_1 - t_2) \, U_{m0;\, m1::n1;\, k\alpha}(\tau)\, \rho_{n2;\, k\alpha}(t_1).$$

$$(D14)$$

Thus

$$S(\omega)_{t_1 \geqslant t_2} = \frac{R_2^2}{\hbar^2} \sum_m \sum_n \sum_{k\alpha} \int_0^\infty dt_2 \int_0^\infty d\tau \, \exp(i\omega\tau)\, U_{m2;\, m1::k\alpha;\, n1}(\tau)\, \rho_{k\alpha;\, n2}(t_2)$$

$$+ \frac{R_1^2}{\hbar^2} \sum_m \sum_n \sum_{k\alpha} \int_0^\infty dt_2 \int_0^\infty d\tau \, \exp(i\omega\tau)\, U_{m1;\, m0::k\alpha;\, n0}(\tau)\, \rho_{k\alpha;\, n1}(t_2)$$

$$+ \frac{R_2 R_1}{\hbar^2} \sum_m \sum_n \sum_{k\alpha} \int_0^\infty dt_2 \int_0^\infty d\tau \, \exp(i\omega\tau)\, U_{m1;\, m0::k\alpha;\, n1}(\tau)\, \rho_{k\alpha;\, n2}(t_2)$$

$$+ \frac{R_1 R_2}{\hbar^2} \sum_m \sum_n \sum_{k\alpha} \int_0^\infty dt_2 \int_0^\infty d\tau \, \exp(i\omega\tau)\, U_{m2;\, m1::k\alpha;\, n0}(\tau)\, \rho_{k\alpha;\, n1}(t_2)$$

$$(D15)$$

$$S(\omega)_{t_2 \geqslant t_1} = \frac{R_2^2}{\hbar^2} \sum_m \sum_n \sum_{k\alpha} \int_0^\infty dt_1 \int_0^\infty d\tau \, \exp(-i\omega\tau)\, U_{m1;\, m2::n1;\, k\alpha}(\tau)\, \rho_{n2;\, k\alpha}(t_1)$$

$$+ \frac{R_1^2}{\hbar^2} \sum_m \sum_n \sum_{k\alpha} \int_0^\infty dt_1 \int_0^\infty d\tau \, \exp(-i\omega\tau)\, U_{m0;\, m1::n0;\, k\alpha}(\tau)\, \rho_{n1;\, k\alpha}(t_1)$$

$$+ \frac{R_2 R_1}{\hbar^2} \sum_m \sum_n \sum_{k\alpha} \int_0^\infty dt_1 \int_0^\infty d\tau \, \exp(-i\omega\tau)\, U_{m1;\, m2::n0;\, k\alpha}(\tau)\, \rho_{n1;\, k\alpha}(t_1)$$

$$+ \frac{R_1 R_2}{\hbar^2} \sum_m \sum_n \sum_{k\alpha} \int_0^\infty dt_1 \int_0^\infty d\tau \, \exp(-i\omega\tau)\, U_{m0;\, m1::n1;\, k\alpha}(\tau)\, \rho_{n2;\, k\alpha}(t_1).$$

$$(D16)$$

To obtain the last expressions, the integration variables   have been changed in the first region $(t_1 \geqslant t_2)$ to τ, t_2 via

the transformation $t_1 = \tau + t_2, t_2 = t_2$ (so the Jacobian equals $+1$) and in the second region ($t_2 \geqslant t_1$) to t_1, τ via the transformation $t_1 = t_1, t_2 = \tau + t_1$ (so the Jacobian equals $+1$).

Since by taking the complex conjugate of the density matrix equations we have

$$\rho_{k\alpha;\, n\nu}(t) = \rho_{n\nu;\, k\alpha}(t)^* \qquad (D17)$$
$$U_{m\lambda;\, \overline{m-1}\lambda::k\alpha;\, \overline{n-1}\nu}(\tau) = U_{\overline{m-1}\lambda;\, m\lambda::\overline{n-1}\nu;\, k\alpha}(\tau) \quad(D18)$$

it is not difficult to see that the terms in the last equation occur in complex conjugate pairs, thus proving that our result for the spectrum is real.

Hence we find that

$$
\begin{aligned}
S(\omega) = \; & 2\,\mathrm{Re}\,\frac{R_2^2}{\hbar^2} \sum_m \sum_n \sum_{k\alpha} \int_0^\infty dt_2 \int_0^\infty d\tau \, \exp(i\omega\tau)\, U_{m2;\, m1::k\alpha;\, n1}(\tau)\, \rho_{k\alpha;\, n2}(t_2) \\
& + 2\,\mathrm{Re}\,\frac{R_1^2}{\hbar^2} \sum_m \sum_n \sum_{k\alpha} \int_0^\infty dt_2 \int_0^\infty d\tau \, \exp(i\omega\tau)\, U_{m1;\, m0::k\alpha;\, n0}(\tau)\, \rho_{k\alpha;\, n1}(t_2) \\
& + 2\,\mathrm{Re}\,\frac{R_2 R_1}{\hbar^2} \sum_m \sum_n \sum_{k\alpha} \int_0^\infty dt_2 \int_0^\infty d\tau \, \exp(i\omega\tau)\, U_{m1;\, m0::k\alpha;\, n1}(\tau)\, \rho_{k\alpha;\, n2}(t_2) \\
& + 2\,\mathrm{Re}\,\frac{R_1 R_2}{\hbar^2} \sum_m \sum_n \sum_{k\alpha} \int_0^\infty dt_2 \int_0^\infty d\tau \, \exp(i\omega\tau)\, U_{m2;\, m1::k\alpha;\, n0}(\tau)\, \rho_{k\alpha;\, n1}(t_2).
\end{aligned}
$$
$$(D19)$$

For each contribution the double integrals factorise, each giving a Laplace transform—albeit for s on the imaginary axis (which may need to be written as a limiting process). We find that

$$
\begin{aligned}
S(\omega) = \; & 2\,\mathrm{Re}\,\frac{R_2^2}{\hbar^2} \sum_m \sum_n \sum_{k\alpha} \widetilde{U}_{m2;\, m1::k\alpha;\, n1}(-i\omega + \epsilon)\, \widetilde{\rho}_{k\alpha;\, n2}(\epsilon') \\
& + 2\,\mathrm{Re}\,\frac{R_1^2}{\hbar^2} \sum_m \sum_n \sum_{k\alpha} \widetilde{U}_{m1;\, m0::k\alpha;\, n0}(-i\omega + \epsilon)\, \widetilde{\rho}_{k\alpha;\, n1}(\epsilon') \\
& + 2\,\mathrm{Re}\,\frac{R_2 R_1}{\hbar^2} \sum_m \sum_n \sum_{k\alpha} \widetilde{U}_{m1;\, m0::k\alpha;\, n1}(-i\omega + \epsilon)\, \widetilde{\rho}_{k\alpha;\, n2}(\epsilon') \\
& + 2\,\mathrm{Re}\,\frac{R_1 R_2}{\hbar^2} \sum_m \sum_n \sum_{k\alpha} \widetilde{U}_{m2;\, m1::k\alpha;\, n0}(-i\omega + \epsilon)\, \widetilde{\rho}_{k\alpha;\, n1}(\epsilon'),
\end{aligned}
$$
$$(D20)$$

where the limits $\epsilon, \epsilon' \to 0$ are understood.

The initial conditions will lead to restrictions on the terms to be summed over. Of course the quantity α already only sums over the three atomic states. As shown previously for the present initial conditions, the only $\rho_{k\alpha;\, n2}(t)$ and $\rho_{k\alpha;\, n1}(t)$ that could be non-zero are those in the $(2,2)$, $(1,1)$ and $(0,0)$ coupled sets—for $(2,2)$ these are $\rho_{02;\, 02}$, $\rho_{02;\, 11}$, $\rho_{02;\, 20}$, $\rho_{11;\, 02}$, $\rho_{11;\, 11}$, $\rho_{11;\, 20}$, $\rho_{20;\, 02}$, $\rho_{20;\, 11}$ and $\rho_{20;\, 20}$; for the $(1,1)$ set we have $\rho_{01;\, 01}, \rho_{01;\, 10}, \rho_{10;\, 01}$ and $\rho_{10;\, 10}$ and for the $(0,0)$ set we have $\rho_{00;\, 00}(t)$—corresponding to the system states $|0;2\rangle$, $|1;1\rangle$ and $|0;1\rangle$ being the only ones populated dur-ing the decay process. The only non-zero elements of the form $\rho_{k\alpha;\, n2}(t)$ are $\rho_{02;\, 02}$, $\rho_{11;\, 02}$ and $\rho_{20;\, 02}$ from the $(2,2)$ set. The only non-zero elements of the form $\rho_{k\alpha;\, n1}(t)$ are $\rho_{02;\, 11}$, $\rho_{11;\, 11}$ and $\rho_{20;\, 11}$ from the $(2,2)$ set and $\rho_{01;\, 01}$ and $\rho_{10;\, 01}$ from the $(1,1)$ set. No elements from the $(0,0)$ set are involved. Only the Laplace transforms of these elements will appear in the expression for the spectrum, and this restricts the related values of k, α and n. The first and third terms in the last expression for the spectrum will thus give three different k, α and n contributions, whilst the second and fourth terms will give five. Thus we may write

$$S(\omega) = S_{22}(\omega) + S_{11}(\omega) + S_{21}(\omega) + S_{12}(\omega) \qquad (D21)$$

$$S_{22}(\omega) = 2\,\mathrm{Re}\,\frac{R_2^2}{\hbar^2}\sum_m \quad [\widetilde{U}_{m2;\,m1::20;\,01}(-i\omega+\epsilon)\,\widetilde{\rho}_{20;\,02}(\epsilon') + \widetilde{U}_{m2;\,m1::11;\,01}(-i\omega+\epsilon)\,\widetilde{\rho}_{11;\,02}(\epsilon')$$

$$+\widetilde{U}_{m2;\,m1::02;\,01}(-i\omega+\epsilon)\,\widetilde{\rho}_{02;\,02}(\epsilon')] \tag{D22}$$

$$S_{11}(\omega) = 2\,\mathrm{Re}\,\frac{R_1^2}{\hbar^2}\sum_m \quad [\widetilde{U}_{m1;\,m0::02;\,10}(-i\omega+\epsilon)\,\widetilde{\rho}_{02;\,11}(\epsilon') + \widetilde{U}_{m1;\,m0::11;\,10}(-i\omega+\epsilon)\,\widetilde{\rho}_{11;\,11}(\epsilon')$$

$$+\widetilde{U}_{m1;\,m0::20;\,10}(-i\omega+\epsilon)\,\widetilde{\rho}_{20;\,11}(\epsilon') + \widetilde{U}_{m1;\,m0::01;\,00}(-i\omega+\epsilon)\,\widetilde{\rho}_{01;\,01}(\epsilon')$$

$$+\widetilde{U}_{m1;\,m0::10;\,00}(-i\omega+\epsilon)\,\widetilde{\rho}_{10;\,01}(\epsilon')] \tag{D23}$$

$$S_{21}(\omega) = 2\,\mathrm{Re}\,\frac{R_2 R_1}{\hbar^2}\sum_m \quad [\widetilde{U}_{m1;\,m0::02;\,01}(-i\omega+\epsilon)\,\widetilde{\rho}_{02;\,02}(\epsilon') + \widetilde{U}_{m1;\,m0::11;\,01}(-i\omega+\epsilon)\,\widetilde{\rho}_{11;\,02}(\epsilon')$$

$$+\widetilde{U}_{m1;\,m0::20;\,01}(-i\omega+\epsilon)\,\widetilde{\rho}_{20;\,02}(\epsilon')] \tag{D24}$$

$$S_{12}(\omega) = 2\,\mathrm{Re}\,\frac{R_1 R_2}{\hbar^2}\sum_m \quad [\widetilde{U}_{m2;\,m1::02;\,10}(-i\omega+\epsilon)\,\widetilde{\rho}_{02;\,11}(\epsilon') + \widetilde{U}_{m2;\,m1::11;\,10}(-i\omega+\epsilon)\,\widetilde{\rho}_{11;\,11}(\epsilon')$$

$$+\widetilde{U}_{m2;\,m1::20;\,10}(-i\omega+\epsilon)\,\widetilde{\rho}_{20;\,11}(\epsilon')$$

$$+\widetilde{U}_{m2;\,m1::01;\,00}(-i\omega+\epsilon)\,\widetilde{\rho}_{01;\,01}(\epsilon') + \widetilde{U}_{m2;\,m1::10;\,00}(-i\omega+\epsilon)\,\widetilde{\rho}_{10;\,01}(\epsilon')]. \tag{D25}$$

This result can be rewritten to group separately the terms where the $\widetilde{\rho}$ are from the $(2,2)$ from those from the $(1,1)$ set:

$$S(\omega) \;=\; S_2'(\omega) + S_6'(\omega) \tag{D26}$$

$$S_2'(\omega) = 2\,\mathrm{Re}\,\frac{R_1^2}{\hbar^2}\sum_m \quad [\widetilde{U}_{m1;\,m0::01;\,00}(-i\omega+\epsilon)\,\widetilde{\rho}_{01;\,01}(\epsilon') + \widetilde{U}_{m1;\,m0::10;\,00}(-i\omega+\epsilon)\,\widetilde{\rho}_{10;\,01}(\epsilon')]$$

$$+2\,\mathrm{Re}\,\frac{R_1 R_2}{\hbar^2}\sum_m \quad [\widetilde{U}_{m2;\,m1::01;\,00}(-i\omega+\epsilon)\,\widetilde{\rho}_{01;\,01}(\epsilon') + \widetilde{U}_{m2;\,m1::10;\,00}(-i\omega+\epsilon)\,\widetilde{\rho}_{10;\,01}(\epsilon')] \tag{D27}$$

$$S_6'(\omega) = 2\,\mathrm{Re}\,\frac{R_2^2}{\hbar^2}\sum_m \quad [\widetilde{U}_{m2;\,m1::20;\,01}(-i\omega+\epsilon)\,\widetilde{\rho}_{20;\,02}(\epsilon')$$

$$+\widetilde{U}_{m2;\,m1::11;\,01}(-i\omega+\epsilon)\,\widetilde{\rho}_{11;\,02}(\epsilon') + \widetilde{U}_{m2;\,m1::02;\,01}(-i\omega+\epsilon)\,\widetilde{\rho}_{02;\,02}(\epsilon')]$$

$$+2\,\mathrm{Re}\,\frac{R_1^2}{\hbar^2}\sum_m \quad [\widetilde{U}_{m1;\,m0::02;\,10}(-i\omega+\epsilon)\,\widetilde{\rho}_{02;\,11}(\epsilon') + \widetilde{U}_{m1;\,m0::11;\,10}(-i\omega+\epsilon)\,\widetilde{\rho}_{11;\,11}(\epsilon')$$

$$+\widetilde{U}_{m1;\,m0::20;\,10}(-i\omega+\epsilon)\,\widetilde{\rho}_{20;\,11}(\epsilon')]$$

$$+2\,\mathrm{Re}\,\frac{R_2 R_1}{\hbar^2}\sum_m \quad [\widetilde{U}_{m1;\,m0::02;\,01}(-i\omega+\epsilon)\,\widetilde{\rho}_{02;\,02}(\epsilon') + \widetilde{U}_{m1;\,m0::11;\,01}(-i\omega+\epsilon)\,\widetilde{\rho}_{11;\,02}(\epsilon')$$

$$+\widetilde{U}_{m1;\,m0::20;\,01}(-i\omega+\epsilon)\,\widetilde{\rho}_{20;\,02}(\epsilon')]$$

$$+2\,\mathrm{Re}\,\frac{R_1 R_2}{\hbar^2}\sum_m \quad [\widetilde{U}_{m2;\,m1::02;\,10}(-i\omega+\epsilon)\,\widetilde{\rho}_{02;\,11}(\epsilon')$$

$$+\widetilde{U}_{m2;\,m1::11;\,10}(-i\omega+\epsilon)\,\widetilde{\rho}_{11;\,11}(\epsilon') + \widetilde{U}_{m2;\,m1::20;\,10}(-i\omega+\epsilon)\,\widetilde{\rho}_{20;\,11}(\epsilon')]. \tag{D28}$$

The $S_2'(\omega)$ terms involve $\widetilde{U}$ of the form $\widetilde{U}_{n,m::1,0}$ since $\rho_{01;\,00}$ and $\rho_{10;\,00}$ are both in the $(1,0)$ set. From

the discussion for the Case A spectrum the only non-zero $\widetilde{U}_{n,m::1,0}$ are of the form $\widetilde{U}_{1,0::1,0}$. Since there are no elements in the $(1,0)$ set of the form $\rho_{m2;\,m1}$ then the second line terms $\widetilde{U}_{m2;\,m1::01;\,00}(-i\omega + \epsilon)$ and $\widetilde{U}_{m2;\,m1::10;\,00}(-i\omega + \epsilon)$ are both zero. As the only element in the $(1,0)$ set of the form $\rho_{m1;\,m0}$ is $\rho_{01;\,00}$ then the first line terms only involve one value of m, which is 0. This gives

$$S_2'(\omega) = 2\,\mathrm{Re}\,\frac{R_1^2}{\hbar^2}[\widetilde{U}_{01;\,00::01;\,00}(-i\omega + \epsilon)\,\widetilde{\rho}_{01;\,01}(\epsilon')$$
$$+\widetilde{U}_{01;\,00::10;\,00}(-i\omega + \epsilon)\,\widetilde{\rho}_{10;\,01}(\epsilon')].$$
$$(D29)$$

The $S_6'(\omega)$ terms involve $\widetilde{U}$ of the form $\widetilde{U}_{n,m::2,1}$ since $\rho_{20;\,01}$, $\rho_{11;\,01}$, $\rho_{02;\,01}$, $\rho_{02;\,10}$, $\rho_{11;\,10}$, $\rho_{20;\,10}$, $\rho_{02;\,01}$, $\rho_{11;\,01}$, $\rho_{20;\,01}$, $\rho_{02;\,10}$, $\rho_{11;\,10}$ and $\rho_{20;\,10}$ all in the $(2,1)$ set (three repeated terms). From the discussion for the Case A spectrum the only non-zero $\widetilde{U}_{n,m::2,1}$ are of the form

$\widetilde{U}_{2,1::2,1}$ and $\widetilde{U}_{1,0::2,1}$. Now in the $(1,0)$ set there are no elements of the form $\rho_{m2;\,m1}$, and the only element of the form $\rho_{m1;\,m0}$ is $\rho_{01;\,00}$. However in the $(2,1)$ set there is one element of the form $\rho_{m2;\,m1}$—which is $\rho_{02;\,01}$, and there is also one element of the form $\rho_{m1;\,m0}$—which is $\rho_{11;\,10}$. Thus the first and fourth lines for $S_6'(\omega)$ will only involve single $\widetilde{U}$, namely $\widetilde{U}_{02;\,01::20;\,01}(-i\omega + \epsilon)$, $\widetilde{U}_{02;\,01::11;\,01}(-i\omega + \epsilon)$ and $\widetilde{U}_{02;\,01::02;\,01}(-i\omega + \epsilon)$ in the first line, and $\widetilde{U}_{02;\,01::02;\,10}(-i\omega + \epsilon)$, $\widetilde{U}_{02;\,01::11;\,10}(-i\omega + \epsilon)$ and $\widetilde{U}_{02;\,01::20;\,10}(-i\omega + \epsilon)$ in the fourth line. However, in the second and third lines two $\widetilde{U}$ are involved, namely $\widetilde{U}_{01;\,00::02;\,10}(-i\omega + \epsilon)$, $\widetilde{U}_{01;\,00::11;\,10}(-i\omega + \epsilon)$ and $\widetilde{U}_{01;\,00::20;\,10}(-i\omega + \epsilon)$ or $\widetilde{U}_{11;\,10::02;\,10}(-i\omega + \epsilon)$, $\widetilde{U}_{11;\,10::11;\,10}(-i\omega + \epsilon)$ and $\widetilde{U}_{11;\,10::20;\,10}(-i\omega + \epsilon)$ for the second line, and $\widetilde{U}_{01;\,00::02;\,01}(-i\omega + \epsilon)$, $\widetilde{U}_{01;\,00::11;\,01}(-i\omega + \epsilon)$ and $\widetilde{U}_{01;\,00::20;\,01}(-i\omega + \epsilon)$ or $\widetilde{U}_{11;\,10::02;\,01}(-i\omega + \epsilon)$, $\widetilde{U}_{11;\,10::11;\,01}(-i\omega + \epsilon)$ and $\widetilde{U}_{11;\,10::20;\,01}(-i\omega + \epsilon)$ for the third line. This gives

$$S_6'(\omega) = 2\,\mathrm{Re}\,\frac{R_2^2}{\hbar^2}\ [\widetilde{U}_{02;\,01::20;\,01}(-i\omega + \epsilon)\,\widetilde{\rho}_{20;\,02}(\epsilon') + \widetilde{U}_{02;\,01::11;\,01}(-i\omega + \epsilon)\,\widetilde{\rho}_{11;\,02}(\epsilon') + \widetilde{U}_{02;\,01::02;\,01}(-i\omega + \epsilon)\,\widetilde{\rho}_{02;\,02}(\epsilon')]$$

$$+2\,\mathrm{Re}\,\frac{R_1^2}{\hbar^2}\ [\{\widetilde{U}_{01;\,00::02;\,10}(-i\omega + \epsilon) + \widetilde{U}_{11;\,10::02;\,10}(-i\omega + \epsilon)\}\,\widetilde{\rho}_{02;\,11}(\epsilon')$$

$$+\{\widetilde{U}_{01;\,00::11;\,10}(-i\omega + \epsilon) + \widetilde{U}_{11;\,10::11;\,10}(-i\omega + \epsilon)\}\,\widetilde{\rho}_{11;\,11}(\epsilon')$$

$$+\{\widetilde{U}_{01;\,00::20;\,10}(-i\omega + \epsilon) + \widetilde{U}_{11;\,10::20;\,10}(-i\omega + \epsilon)\}\,\widetilde{\rho}_{20;\,11}(\epsilon')]$$

$$+2\,\mathrm{Re}\,\frac{R_2 R_1}{\hbar^2}\ [\{\widetilde{U}_{01;\,00::02;\,01}(-i\omega + \epsilon) + \widetilde{U}_{11;\,10::02;\,01}(-i\omega + \epsilon)\}\,\widetilde{\rho}_{02;\,02}(\epsilon')$$

$$+\{\widetilde{U}_{01;\,00::11;\,01}(-i\omega + \epsilon) + \widetilde{U}_{11;\,10::11;\,01}(-i\omega + \epsilon)\}\,\widetilde{\rho}_{11;\,02}(\epsilon')$$

$$+\{\widetilde{U}_{01;\,00::20;\,01}(-i\omega + \epsilon) + \widetilde{U}_{11;\,10::20;\,01}(-i\omega + \epsilon)\}\,\widetilde{\rho}_{20;\,02}(\epsilon')]$$

$$+2\,\mathrm{Re}\,\frac{R_1 R_2}{\hbar^2}\ [\widetilde{U}_{02;\,01::02;\,10}(-i\omega + \epsilon)\,\widetilde{\rho}_{02;\,11}(\epsilon') + \widetilde{U}_{02;\,01::11;\,10}(-i\omega + \epsilon)\,\widetilde{\rho}_{11;\,11}(\epsilon')$$

$$+\widetilde{U}_{02;\,01::20;\,10}(-i\omega + \epsilon)\,\widetilde{\rho}_{20;\,11}(\epsilon')].$$
$$(D30)$$

Combining the results for $S_2'(\omega)$ and $S_6'(\omega)$ we obtain for the spectrum

$$S(\omega) = 2\,\mathrm{Re}\,\frac{R_2^2}{\hbar^2}\ [\widetilde{U}_{02;\,01::20;\,01}(-i\omega + \epsilon)\,\widetilde{\rho}_{20;\,02}(\epsilon') + \widetilde{U}_{02;\,01::11;\,01}(-i\omega + \epsilon)\,\widetilde{\rho}_{11;\,02}(\epsilon') + \widetilde{U}_{02;\,01::02;\,01}(-i\omega + \epsilon)\,\widetilde{\rho}_{02;\,02}(\epsilon')]$$

$$+2\,\mathrm{Re}\,\frac{R_1^2}{\hbar^2}\ [\widetilde{U}_{01;\,00::01;\,00}(-i\omega + \epsilon)\,\widetilde{\rho}_{01;\,01}(\epsilon') + \widetilde{U}_{01;\,00::10;\,00}(-i\omega + \epsilon)\,\widetilde{\rho}_{10;\,01}(\epsilon')$$

$$+\{\widetilde{U}_{01;\,00::02;\,10}(-i\omega + \epsilon) + \widetilde{U}_{11;\,10::02;\,10}(-i\omega + \epsilon)\}\,\widetilde{\rho}_{02;\,11}(\epsilon')$$

$$+\{\widetilde{U}_{01;\,00::11;\,10}(-i\omega + \epsilon) + \widetilde{U}_{11;\,10::11;\,10}(-i\omega + \epsilon)\}\,\widetilde{\rho}_{11;\,11}(\epsilon')$$

$$+\{\widetilde{U}_{01;\,00::20;\,10}(-i\omega + \epsilon) + \widetilde{U}_{11;\,10::20;\,10}(-i\omega + \epsilon)\}\,\widetilde{\rho}_{20;\,11}(\epsilon')]$$

$$+2\,\mathrm{Re}\,\frac{R_2 R_1}{\hbar^2}\ [\{\widetilde{U}_{01;\,00::02;\,01}(-i\omega + \epsilon) + \widetilde{U}_{11;\,10::02;\,01}(-i\omega + \epsilon)\}\,\widetilde{\rho}_{02;\,02}(\epsilon')$$

$$+\{\widetilde{U}_{01;\,00::11;\,01}(-i\omega + \epsilon) + \widetilde{U}_{11;\,10::11;\,01}(-i\omega + \epsilon)\}\,\widetilde{\rho}_{11;\,02}(\epsilon')$$

$$+\{\widetilde{U}_{01;\,00::20;\,01}(-i\omega + \epsilon) + \widetilde{U}_{11;\,10::20;\,01}(-i\omega + \epsilon)\}\,\widetilde{\rho}_{20;\,02}(\epsilon')]$$

$$+2\,\mathrm{Re}\,\frac{R_1 R_2}{\hbar^2}\ [\widetilde{U}_{02;\,01::02;\,10}(-i\omega + \epsilon)\,\widetilde{\rho}_{02;\,11}(\epsilon') + \widetilde{U}_{02;\,01::11;\,10}(-i\omega + \epsilon)\,\widetilde{\rho}_{11;\,11}(\epsilon')$$

$$+\widetilde{U}_{02;\,01::20;\,10}(-i\omega + \epsilon)\,\widetilde{\rho}_{20;\,11}(\epsilon')].$$
$$(D31)$$

REFERENCES

[1] E. M. Purcell, Phys. Rev. **69** 681 (1946).

[2] P.R. Berman, editor. *Cavity Quantum Electrodynamics,* (Academic Press, New York, 1994).

[3] P. Lambropoulos, G.M. Nikolopoulos, T.R. Nielsen and S. Bay, Rep. Prog. Phys. **63** 455 (2000).

[4] H. Walther, B.T.H. Varcoe, B-G. Englert and T. Becker, Rep. Prog. Phys. **69** 1325 (2006).

[5] V. Weisskopf and E. Wigner, Z. Phys. **63** 54 (1930).

[6] E.T. Jaynes and F.W. Cummings, Proc. Inst. Elect. Eng. **51** 89 (1963).

[7] C. Cohen-Tannoudji, in *Frontiers in Laser Spectroscopy*, eds. R. Balian, S. Haroche and S. Liberman (North-Holland, Amsterdam, 1977), Vol. 1, p1.

[8] J.J. Sanchez-Mondragon, N.B. Narozhny and J.H. Eberly, Phys. Rev. Lett. **51** 550 (1983).

[9] J.H. Eberly and K. Wodkiewicz, J. Opt. Soc. Amer. B **2** 1252 (1977).

[10] G.S. Agarwal and R.R. Puri, Phys. Rev. A **33**, 1757 (1986).

[11] M. Lewenstein, J. Zakrzewski and T. Mossberg, Phys. Rev. A **38** 808 (1988).

[12] M. Lax, Phys. Rev. **129**, 2342 (1963), *ibid.* Phys. Rev. **157** 213 (1967).

[13] H.J. Carmichael, R.J. Brecha, M.G. Raizen, H.J. Kimble and P.R. Rice, Phys. Rev. A **40** 5516 (1991).

[14] J.J. Childs, K. An, R.R. Dasari and M.S. Feld, in *Cavity Quantum Electrodynamics,* edited by P.R. Berman (Academic Press, New York, 1994), p.325.

[15] H.J. Carmichael, L. Tian, W. Ren and P. Alsing, in *Cavity Quantum Electrodynamics,* edited by P.R. Berman (Academic Press, New York, 1994), p.381.

[16] R.J. Thompson, G. Rempe and H.J. Kimble, Phys. Rev. Lett. **68** 1132 (1992).

[17] A. Boca, R. Miller, K.M. Birnbaum, A.D. Boozer, J. McKeever and H.J. Kimble. Phys. Rev. Lett. **93** 233603 (2004).

[18] M. Brune, F. Schmidt-Kaler, A. Maali, J. Dreyer, E. Hagley, J.M. Raimond and S. Haroche. Phys. Rev. Lett. **76** 1800 (1996).

[19] G. Rempe, H. Walther and N. Klein, Phys. Rev. Lett. **58** 353 (1987).

[20] J.H. Eberly, N.B. Narozhny and J.J. Sanchez-Mondragon. Phys. Rev. Lett. **44** 1323 (1980).

[21] S.M. Barnett and P.L. Knight, Phys. Rev. A **33** 2444 (1986).

[22] B.R. Mollow, Phys. Rev **188** 1969 (1969), *ibid.* Phys. Rev. A **5** 2217 (1972).

[23] G.S. Agarwal, R.K. Bullough and N. Nayak, Opt. Comm. **85** 202 (1991).

[24] S. John and T. Quang, Phys. Rev. A **50** 1764 (1994).

[25] M.M. Ashraf, Phys. Rev. A **50** 741 (1994).

[26] S. Bay and P. Lambropoulos, Opt. Comm. **146** 130 (1998).

[27] E. Paspalakis, D.G. Angelakis and P.L. Knight, .Opt. Comm. **172** 229 (1999).

[28] Q-C. Zhou, S-N. Zhu and N-B Ming, J. Phys. B: At. Mol. Opt. Phys. **38** 4309 (2005).

[29] B.M. Garraway and B.J Dalton, J. Phys. B: At. Mol. Opt. Phys. **39** S767 (2006).

[30] B.J. Dalton, S.M. Barnett and B.M. Garraway, Phys. Rev. A **64** 053813 (2001).

[31] S. Swain and Z. Ficek, editors. Special Issue: *Quantum Interference.* J. Mod. Opt. **49** 1/2 (2002).

[32] R.J. Glauber, in *Quantum Optics and Electronics*, edited by C. DeWitt, A. Blandin and C. Cohen-Tannoudji (Gordon and Breach, London, 1965), p65.

[33] J.D. Cresser, Phys. Rep. **94** 47 (1983).

[34] B.J. Dalton, S.M. Barnett and P.L. Knight, J. Mod. Opt. **46** 1315 (1999).

[35] S. Brown and B.J. Dalton, J. Mod. Opt. **48** 597 (2001).

[36] B.J. Dalton, E.S. Guerra and P.L. Knight, Phys. Rev. A **54** 2292 (1996).

[37] B.J. Dalton and M. Babiker, Phys. Rev. A **56** 905 (1997).

[38] W.H. Louisell, *Quantum Statistical Properties of Radiation* (Wiley, New York, 1973), p57.

[39] I.E. Linington and B.M. Garraway, J. Phys. B: At. Mol. Opt. Phys. **39** 3383 (2006).

[40] D.F. Walls and G.J. Milburn, *Quantum Optics* (Springer-Verlag, Berlin, 1994), p118.

[41] B.J. Dalton, *Lecture Notes in Quantum Optics* (University of Queensland, Brisbane, 1979). Unpublished.